AMERICAN SOCIETY FOR MICROBIOLOGY | Applied and Environmental Microbiology®

ENVIRONMENTAL MICROBIOLOGY

Uptake of Phytoplankton-Derived Carbon and Cobalamins by Novel *Acidobacteria* Genera in *Microcystis* Blooms Inferred from Metagenomic and Metatranscriptomic Evidence

Derek J. Smith,[a] Jenan J. Kharbush,[a] Roland D. Kersten,[b] Gregory J. Dick[a,c]

[a]Department of Earth & Environmental Science, University of Michigan, Ann Arbor, Michigan, USA
[b]Department of Medicinal Chemistry, University of Michigan, Ann Arbor, Michigan, USA
[c]Cooperative Institute for Great Lakes Research, School of Environment and Sustainability, University of Michigan, Ann Arbor, Michigan, USA

ABSTRACT Interactions between bacteria and phytoplankton can influence primary production, community composition, and algal bloom development. However, these interactions are poorly described for many consortia, particularly for freshwater bloom-forming cyanobacteria. Here, we assessed the gene content and expression of two uncultivated *Acidobacteria* from Lake Erie *Microcystis* blooms. These organisms were targeted because they were previously identified as important catalase producers in *Microcystis* blooms, suggesting that they protect *Microcystis* from H_2O_2. Metatranscriptomics revealed that both *Acidobacteria* transcribed genes for uptake of organic compounds that are known cyanobacterial products and exudates, including lactate, glycolate, amino acids, peptides, and cobalamins. Expressed genes for amino acid metabolism and peptide transport and degradation suggest that use of amino acids and peptides by *Acidobacteria* may regenerate nitrogen for cyanobacteria and other organisms. The *Acidobacteria* genomes lacked genes for biosynthesis of cobalamins but expressed genes for its transport and remodeling. This indicates that the *Acidobacteria* obtained cobalamins externally, potentially from *Microcystis*, which has a complete gene repertoire for pseudocobalamin biosynthesis; expressed them in field samples; and produced pseudocobalamin in axenic culture. Both *Acidobacteria* were detected in *Microcystis* blooms worldwide. Together, the data support the hypotheses that uncultured and previously unidentified *Acidobacteria* taxa exchange metabolites with phytoplankton during harmful cyanobacterial blooms and influence nitrogen available to phytoplankton. Thus, novel *Acidobacteria* may play a role in cyanobacterial physiology and bloom development.

IMPORTANCE Interactions between heterotrophic bacteria and phytoplankton influence competition and successions between phytoplankton taxa, thereby influencing ecosystem-wide processes such as carbon cycling and algal bloom development. The cyanobacterium *Microcystis* forms harmful blooms in freshwaters worldwide and grows in buoyant colonies that harbor other bacteria in their phycospheres. Bacteria in the phycosphere and in the surrounding community likely influence *Microcystis* physiology and ecology and thus the development of freshwater harmful cyanobacterial blooms. However, the impacts and mechanisms of interaction between bacteria and *Microcystis* are not fully understood. This study explores the mechanisms of interaction between *Microcystis* and uncultured members of its phycosphere *in situ* with population genome resolution to investigate the cooccurrence of *Microcystis* and freshwater *Acidobacteria* in blooms worldwide.

KEYWORDS *Acidobacteria*, *Microcystis*, cyanobacterial blooms, metagenomics, metatranscriptomics, microbial ecology, phycosphere

Interactions between microorganisms have profound impacts on global biogeochemistry by influencing microbial fitness, metabolism, and community composition. For example, many microbes use the waste products of others for growth or produce

Editor Jennifer B. Glass, Georgia Institute of Technology

Address correspondence to Gregory J. Dick, gdick@umich.edu.

The authors declare no conflict of interest.

For a companion article on this topic, see https://doi.org/10.1128/AEM.02544-21.

Received 20 September 2021
Accepted 17 February 2022
Published 5 July 2022

compounds required by other community members (1–3). A widely recognized example of such metabolic handoffs is in the interactions between phytoplankton and heterotrophic bacteria. Phytoplankton support heterotrophic bacterial growth by providing organic carbon and organic sulfur (4, 5). In addition, some heterotrophic bacteria can obtain cobalamin (vitamin B_{12}) by remodeling pseudocobalamin (6, 7), of which cyanobacteria are a major environmental source (8). In turn, the heterotrophic partners can improve phytoplankton growth by producing essential vitamins and growth factors such as cobalamins (4, 9), increasing the bioavailability of trace metal cofactors (10), regenerating nutrients from organic material (11–13), and detoxifying reactive oxygen species (14). Heterotrophic bacteria are known to impact phytoplankton fitness through the transfer of metabolites (10, 11, 15, 16) in a zone of close physical association termed the phycosphere (17, 18).

Interactions between heterotrophic bacteria and phytoplankton also influence competition between phytoplankton taxa (19). Thus, phycosphere interactions likely play a role in shaping successions of phytoplankton taxa (20) and may have implications at the level of whole ecosystems by modulating primary productivity and phytoplankton bloom formation (16, 18, 21). Interactions in the phycosphere can have both strain- and species-specific outcomes (11, 22), and the fitness impacts on phytoplankton have been linked to the exchange of specific metabolites in some interactions (9, 15, 16). Therefore, identifying the bacterial taxa associated with a given phytoplankton taxon and the metabolites exchanged between them can improve our understanding of phytoplankton physiology and competition between phytoplankton in natural assemblages with cooccurring bacteria, thereby improving modeling of ecosystem-wide processes such as primary productivity and harmful algal bloom formation (16, 18, 21).

Phytoplankton-bacterium interactions likely influence the development and phytoplankton community structure of *Microcystis* blooms, which degrade freshwater systems around the world (23). Metagenomic and metatranscriptomic studies have suggested complementary gene content (24) and expression (25) in *Microcystis* and cooccurring bacterial communities. Furthermore, *Microcystis* spp. grow in colonies that harbor heterotrophic bacterial communities that differ from the surrounding microbial communities (26–28) and differ both seasonally (27) and by *Microcystis* genotype (27, 29). Heterotrophic bacteria have previously been shown to impact competition between *Microcystis* and eukaryotic algae (19). Such impacts on the invasion and successions of phytoplankton taxa are likely important determinants of toxin concentrations in *Microcystis* blooms, which are substantially influenced by the relative proportions of toxin-producing and non-toxin-producing *Microcystis* spp. (30, 31). However, the impact of phycosphere bacteria on *Microcystis* growth and physiology remains uncharacterized, in part because many of the microbes associated with *Microcystis* colonies are yet to be cultured (26, 27, 32) and existing metatranscriptomic studies lack genome-resolved analysis of *in situ* communities (25, 33–35). Direct recovery of bacterial genomes from the environment can provide insights into the biochemical and ecological characteristics of these uncultivated organisms of interest.

This study focused on metagenome-assembled genomes (MAGs) of two novel, uncultivated *Acidobacteria* from a western Lake Erie cyanobacterial harmful algal bloom (CHAB) in the summer-fall of 2014. These *Acidobacteria* were responsible for a substantial fraction of catalase transcripts in a western Lake Erie *Microcystis* bloom community despite their low relative abundance (36). Therefore, both *Acidobacteria* may be important for H_2O_2 detoxification during CHABs, which is an essential service that heterotrophic bacteria provide to some cyanobacterial species (14) and has been proposed to influence *Microcystis* strain succession during CHABs (36). In addition, both genomes were reconstructed from phytoplankton- and particle-attached size fractions, and one of the *Acidobacteria* (genus *Bryobacter*) was previously identified in 25% of individual *Microcystis* colony phycosphere communities (27) and correlated with certain *Microcystis* genotypes (37). Together, these results suggest that the *Acidobacteria* interact with *Microcystis* and other phytoplankton in freshwater cyanobacterial blooms.

Here, we examined the gene content and expression of the *Acidobacteria* MAGs during the western Lake Erie cyanobacterial bloom in the summer-fall of 2014 to

TABLE 1 Quality information for *Acidobacteria* MAGs from western Lake Erie cyanobacterial blooms

BinID	Genus	Completeness (%)	Contamination (%)	GC %	Size (Mbp)	N_{50}	Gene count	16S no.	23S no.	tRNA no.
CoA8 C33	*Bryobacter*	98.21	0.87	60.89	5.0536	7,548	4,488	1	1	47
CoA2 C42	Unclassified	98.70	2.17	64.93	6.0673	38,916	5,163	1	1	47

explore potential interactions with cyanobacteria and other phytoplankton. In addition, the abundance of both *Acidobacteria* in amplicon data sets from size-fractionated samples in a range of eutrophic environments was examined to determine their specificity to cyanobacterial blooms and *Microcystis* colonies. The data suggest that both genomes express genes involved in degradation of exopolysaccharide (EPS), organic acids, amino acids, and peptides but are only occasionally found in *Microcystis* bloom communities.

RESULTS AND DISCUSSION

Identification of two novel species of subdivision 3 *Acidobacteria* in *Microcystis* blooms. Metagenome-assembled genomes (MAGs) of two *Acidobacteria* were obtained from metagenomic data from microbial communities collected during the summer-fall of 2014 (see Data Set S1 in the supplemental material). The samples spanned various environmental conditions and stages of *Microcystis* bloom development (36, 38, 39). These genomes were targeted because they highly expressed catalase-peroxidase genes (*katG*) during the cyanobacterial bloom (36) and were detected in particle- or phytoplankton-attached samples (27, 36) and thus were hypothesized to be associated with phytoplankton and important degraders of H_2O_2, which may influence the composition and development of cyanobacterial blooms (40).

Both genomes are nearly complete with low contamination and meet standards for high-quality draft genomes (Table 1) (41). The 16S rRNA gene sequences of MAGs CoA2 C42 and CoA8 C33 were classified as *Paludibaculum* and *Bryobacter* (see Materials and Methods) and were closest matches to 16S rRNA gene sequences from *Paludibaculum fermentans* and *Bryobacter aggregatus* strains (92.29 and 96.5%, respectively), which were both isolated from peat bogs (42, 43). Based on 16S rRNA gene similarity thresholds for species and genera (44), the percent similarity score for the CoA8 C33 MAG with *Bryobacter aggregatus* is above genus-level thresholds, and the percent similarity for CoA2 C42 MAG with *Paludibaculum fermentans* is below genus-level but above family-level thresholds. Phylogeny of 16S rRNA gene sequences placed both genomes within subdivision 3 *Acidobacteria*, *Bryobacteraceae* (Fig. 1A). While the CoA8 C33 MAG was placed as a sister lineage to *Bryobacter aggregatus* with high confidence, the specific placement of the CoA2 C42 MAG within subdivision 3 *Acidobacteria* had lower bootstrap support. These results support that genome CoA8 C33 is a novel species of *Bryobacter*, while genome CoA2 C42 likely represents a novel genus within the subdivision 3 *Acidobacteria* sister to *Paludibaculum*. Here, these species will be referred to as *Bryobacter* CoA8 C33 and acidobacterium CoA2 C42.

Whole-genome alignments also indicated that both genomes were most similar to *Acidobacteria* genomes from subdivision 3 (Fig. 1B and C). The CoA8 C33 genome was most similar to *Bryobacter aggregatus* strains, with genomic average nucleotide identity (gANI) and alignment coverage values (0.72 and 0.44, respectively) within the range of genus-level but below species-level cutoffs (45, 46), further supporting that it is a novel species of *Bryobacter*. The CoA2 C42 genome was most similar to a MAG from a drinking-water metagenome (IMG Gold Study identifier [ID]: Gs0114768). While subdivision 3 *Acidobacteria* have been recognized as numerically important in soils (47, 48) and present in the microbiome of marine sponges (49), freshwater (37), and marine waters (50), to our knowledge, this study represents the first detailed and targeted description of nearly complete *Bryobacteraceae* genomes from an aquatic environment.

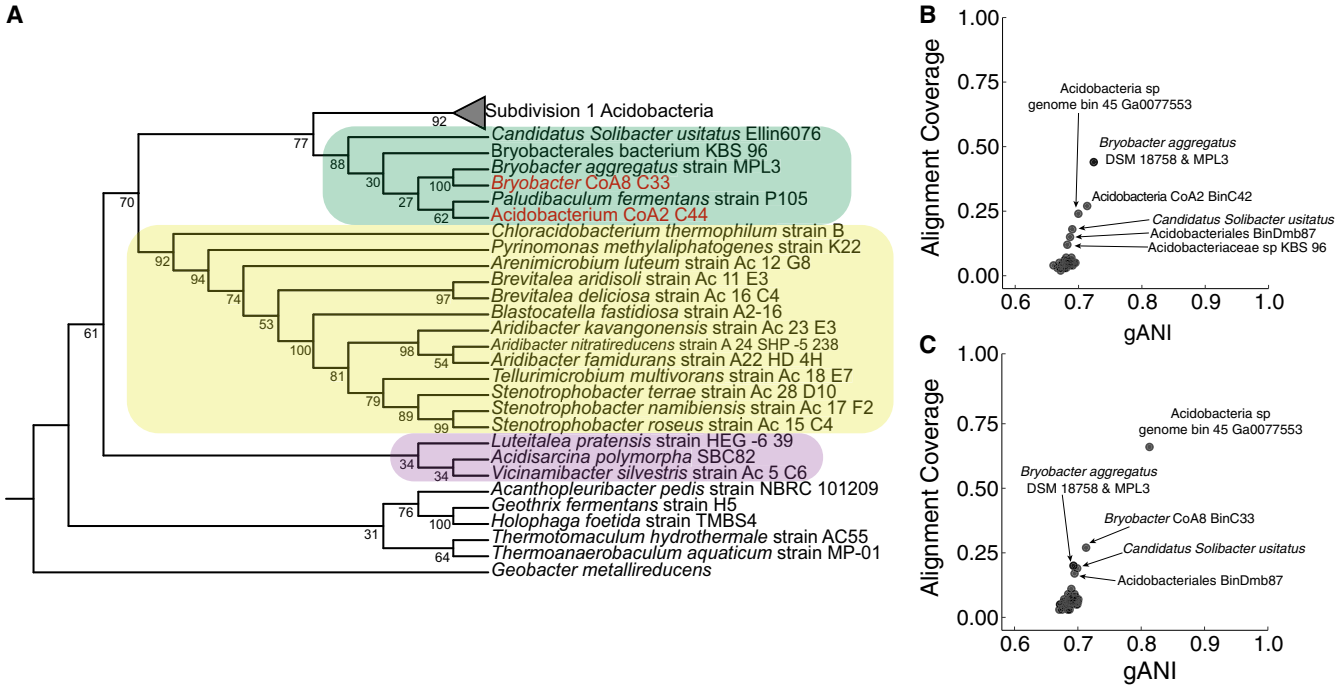

FIG 1 Taxonomic assignment of novel *Acidobacteria* MAGs based on 16S rRNA phylogeny and genomic average nucleotide identity (gANI). (A) Maximum likelihood tree of published, full-length *Acidobacteria* 16S rRNA gene sequences. The tree is rooted with the sequence from the *deltaproteobacterium Geobacter metallireducens*. Node labels show bootstrap support (n = 2,000). Branch lengths have no information. Subdivision 3 *Acidobacteria* are highlighted in green, subdivision 4 *Acidobacteria* are highlighted in gold, and subdivision 6 *Acidobacteria* are highlighted in purple. The leaf labels for the 16S rRNA sequences from the Lake Erie MAGs are colored red. (B and C) gANI comparisons of *Bryobacter* CoA8 C33 (C) and *Acidobacteria* CoA2 C42 (B) with published, high-quality *Acidobacteria* genomes in IMG (n = 63).

Highly expressed genes are involved in ATP synthesis, respiration, biofilm adhesion, and chemotaxis. In both genomes, the most highly expressed genes were involved in translation, secretion proteins, peptidases of unknown function, chaperonins, H_2O_2 detoxification, and ATP synthesis, along with hypothetical or uncharacterized proteins (see Fig. S3 and S4 in the supplemental material). Highly expressed genes encoding hypothetical proteins did not align with RNA gene sequences in NCBI and either had best hits to other hypothetical proteins or no significant hits to any proteins in the database, suggesting that they encode proteins of unknown function (Table S2). Both genomes have a complete tricarboxylic acid (TCA) cycle, cytochrome *c* oxidase, and nearly complete glycolysis and Entner-Doudoroff pathways (Fig. S5) and lack known pathways for carbon fixation and synthesis of bacteriochlorophyll and rhodopsin pigments, indicating that these organisms are aerobic chemoheterotrophs like known subdivision 3 *Acidobacteria* isolates (51). Highly expressed genes involved in biofilm adhesion, chemotaxis, flagellum biosynthesis, and motility (Fig. S6 and S7) indicate that these organisms are chemotactic.

Expression of genes involved in degradation of exopolysaccharides. Functional annotation of expressed genes suggests that both *Acidobacteria* obtain carbon from breakdown of complex exopolysaccharides, including known phytoplankton products. Both genomes possess putative pectate-lyase, alpha-mannosidase, and xylan esterase exoenzymes to completely degrade homogalacturonan, mannose, and xylose polymers completely to the constituent monosaccharides (Fig. S5 and Data Sets S2 and S3 in the supplemental material). The *Bryobacter* MAG also contains genes for degradation of galactose and arabinofuranose polymers, while the *Acidobacteria* CoA2 C42 MAG contains genes for the degradation of alginate (Fig. S5). Both *Acidobacteria* genomes also expressed genes involved in the degradation of galacturonate monomers and other monosaccharides such as xylose, glucose, galactose, and mannose (Fig. S5). These monosaccharides along with uronic acid polymers make up the exopolysaccharide (EPS) mucilage encasing cyanobacterial cells (52–55), and bacterial degradation of

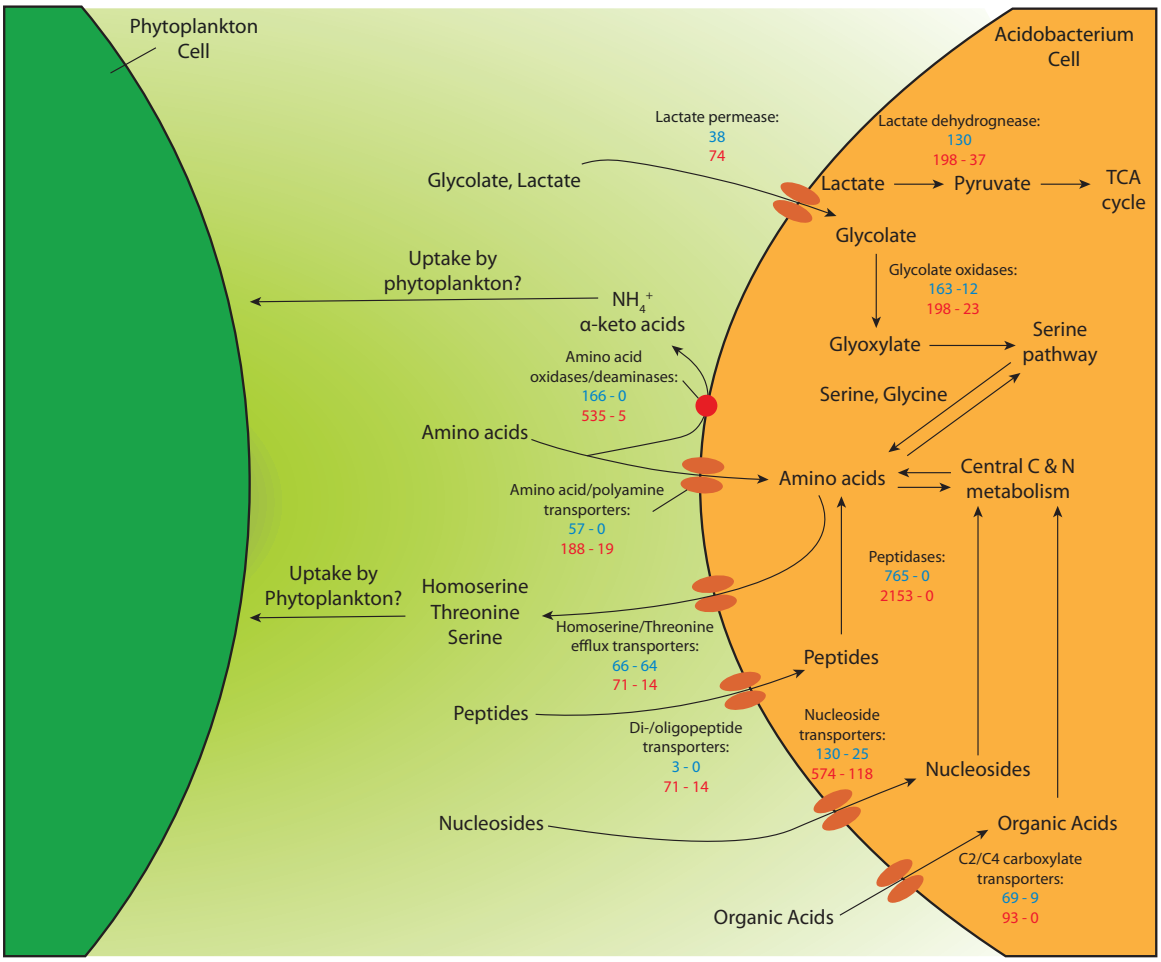

FIG 2 Relative abundance of low-molecular-weight organic carbon transporters and enzymes related to their metabolism by *Bryobacter* CoA8 C33 (blue) and acidobacterium CoA2 C42 (red) associated with phytoplankton seston in the 4 August metatranscriptome from nearshore western Lake Erie station WE12. Relative abundance is expressed as reads mapped per kilobase of gene per million reads mapped to the respective genome (RPKM; rounded to the nearest whole number). A range of RPKM values indicates that multiple gene loci were predicted to encode the indicated reactions (includes gene duplications or genes encoding enzyme subunits), and only maximum and minimum RPKM values are shown.

Microcystis EPS has been observed in cocultures with heterotrophic bacteria (55), supporting the hypothesis that EPS in *Microcystis* colonies could be a substrate of the *Acidobacteria* exoenzymes. Eukaryotic phytoplankton also produce extracellular polysaccharides composed of these same constituents (56–58), which could potentially provide carbon to these organisms (56–59).

Evidence for uptake of low-molecular-weight organic compounds. Metatranscriptomic data suggest that low-molecular-weight organic carbon is a source of carbon and nitrogen for both *Acidobacteria* and further support the hypothesis that both *Acidobacteria* participate in metabolic exchanges within phycosphere communities, which may include phytoplankton and other heterotrophic organisms (Fig. 2). Among the most highly expressed transporters in both *Acidobacteria* during the *Microcystis* bloom were concentrative nucleoside transporters (CNT) (Fig. S6 and S7), suggesting that they use nucleosides from the environment. There was also detectable expression of many genes putatively encoding amino acid, peptide, and polyamine uptake (Fig. 2). This indicates that the nitrogen demand for both *Acidobacteria* is likely met in part by uptake of organic nitrogen in dissolved amino acids, peptides, and nucleosides, which are important sources of nitrogen for bacterioplankton (60–62) and are derived from a wide variety of cell lysates and exudates, including those from phytoplankton (4, 13, 59, 63). Expression of amino acid oxidases (Fig. 2) suggests that both *Acidobacteria* deaminate amino acids to access nitrogen (61, 64, 65).

The metatranscriptomic data also suggest uptake of phytoplankton exudate. Both *Acidobacteria* expressed genes to oxidize lactate and glycolate and dephosphorylate phosphoglycolate (Fig. 2), which are common exudates of cyanobacteria (63, 66, 67) and eukaryotic phytoplankton (68, 69). Lactate permease, which is involved in uptake of both lactate and glycolate (70), was expressed, along with transporters putatively involved in the uptake of other organic acids (Fig. 2). Among the known pathways for glycolate use in bacteria, both genomes lack genes in the glyoxylate cycle and methylaspartate cycle and the majority of genes in the ethylmalonyl coenzyme A (CoA) and 3-hydroxypropanoate cycles but possess and express genes in the serine pathway, although the final two genes of this pathway are missing in both genomes (Fig. 2 and Fig. S8). The presence of genes in the serine pathway perhaps indicates that the glyoxylate formed from the oxidation of glycolate is incorporated into amino acids (71–73) and the metabolism of C_1 compounds (73).

Evidence for regeneration of nitrogen from peptides and amino acids. Transcripts for dipeptide and oligopeptide transporters, peptidases, and cyanophycinase-like proteins suggest that both *Acidobacteria* use extracellular peptides as a carbon and nitrogen source (Fig. 2). Expressed amino acid efflux transporters (Fig. 2) further suggest that peptide degradation may be linked to efflux of excess amino acids. Amino acid efflux allows biosynthesis of other amino acids to meet cellular demands (74–76) and is essential for maintaining balanced growth from degradation of oligopeptides (76–78). Thus, peptide degradation followed by amino acid efflux by bacteria could regenerate amino acids, which have been shown to enhance cyanobacterial growth and biomass in lakes (30) and cyanobacterial cultures (79–81).

Bacteria can also regenerate nitrogen from organic matter via excretion of ammonia when amino acids are the major sources of nitrogen for bacterial growth (60) or under carbon-limiting conditions (82, 83). In both *Acidobacteria*, expression of amino acid oxidases/deaminases (Fig. 2), which convert extracellular amino acids into ammonium, supports that these organisms regenerate ammonia from dissolved amino acids. Ammonium generated from dissolved organic matter (DOM) is used by phytoplankton and bacteria for growth (64, 65), community demand for ammonium can be high in *Microcystis* blooms (84), and ammonium uptake by *Microcystis* has been linked to ammonium regeneration from DOM by cooccurring microbes (25, 84). Together, these data support the hypothesis that bacterial excretion of ammonia is a potential source of nitrogen for Lake Erie cyanobacteria.

Evidence for cobalamin auxotrophy and uptake. Gene annotation and expression data from the *Acidobacteria* genomes suggest that both organisms are auxotrophs of cobalamin. Some cobalamin-dependent enzymes are involved in critical cellular functions such as methionine and nucleotide synthesis (85). Thus, organisms that lack genes for cobalamin biosynthesis must obtain cobalamin released into the environment by cobalamin-producing organisms (9, 86). Both *Acidobacteria* lack the entire pathway for biosynthesis of the corrin ring structure common to all cobalamins, as in other heterotrophic bacteria cocultured with cyanobacteria (87). The *Bryobacter* genome expressed genes annotated as cobalamin transporters (Fig. 3A), but the *Acidobacteria* CoA2 C42 MAG lacked genes annotated as cobalamin transporters (see Data Set S2 in the supplemental material). Both genomes expressed genes encoding TonB-family proteins, which are required to energize the membrane for cobalamin transport (88, 89), and some of these were among the most highly expressed membrane-associated proteins in *Acidobacteria* CoA2 C42 (Fig. S6). Together, this suggests that neither of these *Acidobacteria* can synthesize cobalamins *de novo* and that both transport cobalamins from the environment into the cell.

Both *Acidobacteria* expressed cobalamin-dependent genes. A *nrdJ*-encoded class II ribonucleotide reductase and a *metH*-encoded methionine synthase were detected in the *Bryobacter* genome (Fig. 3B). *Bryobacter* CoA8 C33 lacks cobalamin-independent alternatives to *nrdJ*, which suggests that cobalamin is a requirement for this organism. Although *Acidobacteria* CoA2 C42 uses the cobalamin-independent alternatives to *nrdJ*, *nrdA* and *nrdB* (Data Set S2 in the supplemental material), and has the cobalamin-independent version *metE* (for which no expression was detected), it expressed *metH*

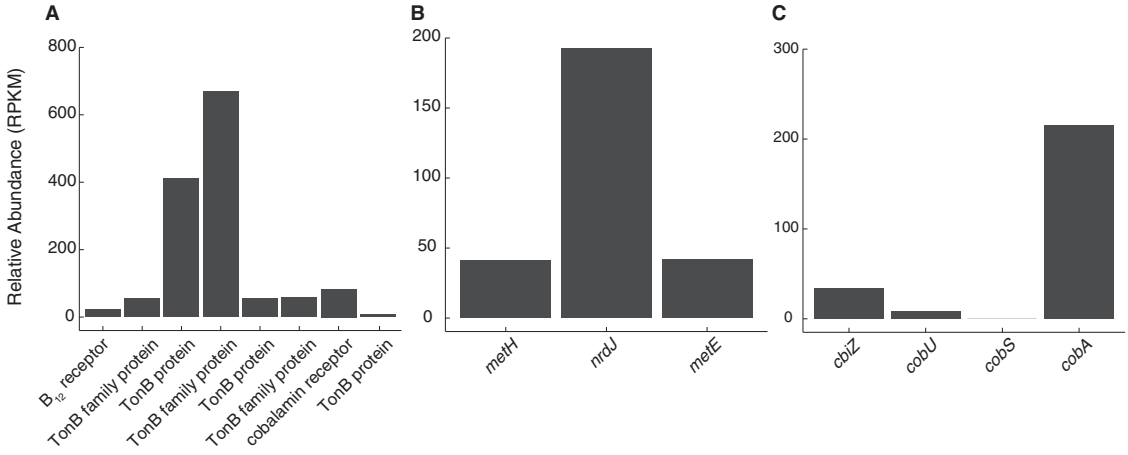

FIG 3 Relative abundance of transcripts from the *Bryobacter* CoA8 C33 genome involved in cobalamin transport (A), cobalamin-dependent genes and their cobalamin-independent counterparts (B), and cobalamin remodeling (C) in the 4 August metatranscriptome from western Lake Erie nearshore station WE12. Relative abundance is expressed as reads mapped per kilobase pair of gene per million reads mapped to the genome (RPKM).

(Table 2). Therefore, both organisms were likely using cobalamins during the cyanobacterial bloom.

We also detected expression of genes involved in remodeling cobalamin axial ligands in both *Acidobacteria* genomes. Variants of cobalamins differ in the chemical groups that make up the upper and lower axial ligands (85, 86), and because most microbial taxa exclusively use cobalamins with specific lower axial ligand structures (8, 86, 90), mechanisms to remodel cobalamins are necessary for microbes to convert the various exogenous cobalamin forms into the correct chemical forms needed for growth (6, 86, 91). Both genomes possessed genes for attaching an adenosyl group to the upper ligand (Fig. 3C and Table 2), but only the *Bryobacter* genome had genes for remodeling the lower axial ligand (Fig. 3C). Expression of cobalamin-remodeling genes in *Bryobacter* suggests that it can convert various chemical forms of cobalamin into the specific variant required as its enzyme cofactor.

We identified methylpseudocobalamin and two stereoisomers of hydroxopseudocobalamin in axenic cultures of *Microcystis aeruginosa* PCC 7806 and PCC 9806 (Fig. 4A; see also Fig. S9 to S11). Cobalamins containing a methyl group in the upper ligand are the active cofactors for methyltransferase reactions, including methionine synthesis (85), whereas cobalamins containing a hydroxyl group in the upper ligand are degradation products of biologically active pseudocobalamins (92). Cyanocobalamin and other forms of cobalamin (the lower axial ligand is 5,6-dimethylbenzimidazol [DMB]) were not detected in *Microcystis* cultures (Fig. 4B), consistent with previous studies of cyanobacteria (8, 86, 93). In addition to detecting pseudocobalamin in *Microcystis* biomass, we detected a complete pathway for production of pseudocobalamin in closed *Microcystis* genomes, which recruited reads at greater than 95% nucleotide identity from western Lake Erie metatranscriptomes (Fig. S12). The presence and expression of complete genetic pathways for pseudocobalamin biosynthesis in *Microcystis* genomes and communities, along with metabolomic analyses, support that *Microcystis* produces methylpseudocobalamin for growth as do other cyanobacteria (8, 86, 87, 94). Taken together with expression of cobalamin-remodeling genes (Fig. 3C) and genes that require cobalamin for nucleotide and methionine synthesis by *Bryobacter* CoA8 C33

TABLE 2 Expression of B_{12}-dependent genes in *Acidobacteria* CoA2 C42 MAG

Gene	KEGG no.	KO	IMG annotation	Gene symbol(s)	4 August RPKM
2806999884	2.1.1.13	K00548	Methionine synthase (B_{12} dependent)	*metH*	216.80
2807002171	2.1.1.14	K00549	5-Methyltetrahydropteroyltriglutamate–homocysteine methyltransferase	*metE*	0
2807000579	2.5.1.17	K00798	Cob(I)alamin adenosyltransferase	*cobA*, *pduO*	93.77

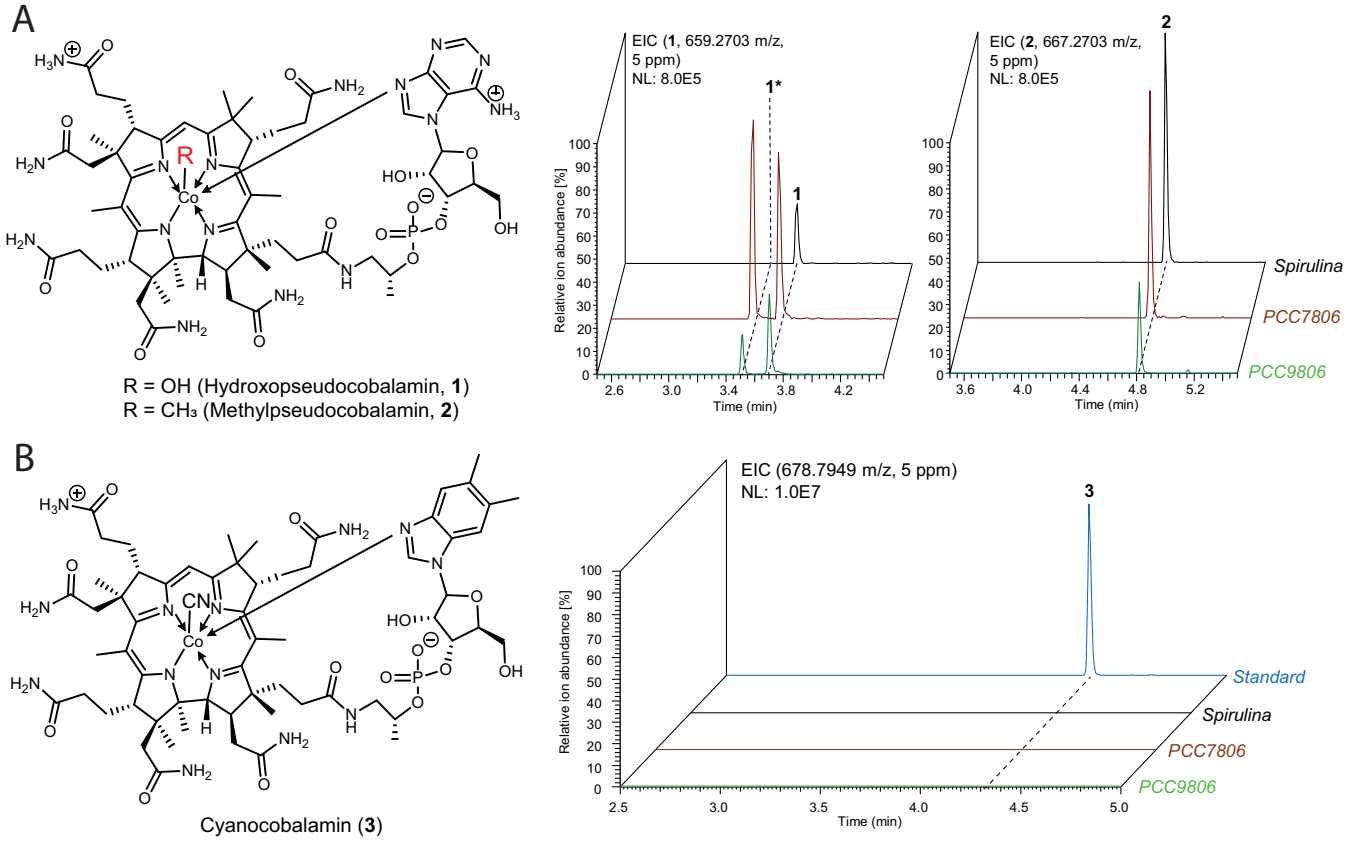

FIG 4 (A) Structure and LC-MS chromatograms of pseudocobalamin forms observed in *Microcystis* cultures and *Spirulina* powder. The *Spirulina* served as a positive control given that commercial standards for pseudocobalamin are not readily available. The compound labeled 1* has the same molecular weight and mass spectrum as compound 1 and is therefore a potential stereoisomer of hydroxopseudocobalamin that was observed only in *Microcystis* cultures. (B) Structure of cyanocobalamin and LC-MS chromatograms of a cyanocobalamin standard compared with *Microcystis* cultures and *Spirulina* powder, demonstrating its absence in the cyanobacterial samples tested here. Arrows indicate metal coordination in cobalamin structures. EIC, extracted ion chromatogram; NL, normalization value for extracted ion intensity.

(Fig. 3B) and the physical association of *Bryobacter* with *Microcystis* phycosphere colonies (27), these results support the hypothesis that *Microcystis* and other bloom-associated cyanobacteria (e.g., *Synechococcus-Cyanobium* [27]) that are known cobalamin producers (8, 94) are potential sources of cobalamins for *Bryobacter* CoA8 C33. The chemical form of cobalamins used by both *Acidobacteria* remains unknown, so it is possible that the *Acidobacteria* obtain cobalamins from other sources (91). Regardless, our data suggest that both *Acidobacteria* rely on other microorganisms to meet cobalamin demands.

Presence and relative abundance in 16S rRNA gene amplicon data sets. To determine if these *Acidobacteria* regularly occur in, or are specific to, *Microcystis*-dominated blooms, we measured their abundance in published 16S rRNA gene amplicon data sets spanning a range of freshwater systems where *Microcystis*-dominated blooms occur (Table 3; see Materials and Methods). Amplicon sequences with high percent similarity (97%) to variable regions of the 16S rRNA gene sequences in both *Acidobacteria* MAGs were present at low relative abundance in western Lake Erie (*Bryobacter*, mean 0.072%, range 0 to 1.41%; acidobacterium CoA2 C42, mean 0.13%, range 0 to 0.69%) and other systems (*Bryobacter*, mean 0.006%, range 0 to 0.40%; acidobacterium CoA2 C42, mean 0.048%, range 0 to 0.72%). There was a weak but significant positive relationship between the relative abundance of both *Acidobacteria* taxa and *Microcystis* relative abundance in whole water samples collected from western Lake Erie cyanobacterial blooms (Fig. 5A and B). In 100-μm retentate samples from the summer-fall of 2014 in western Lake Erie, there were no significant relationships between the relative abundances of *Microcystis* and *Acidobac-*

TABLE 3 Description of public data sets mined for *Acidobacteria* 16S rRNA sequences in this study

NCBI accession no.	Location and sampling scheme	Material type	Size fraction(s)	Reference
PRJNA575023	Discrete sampling of eutrophic lakes around the globe	Bulk phytoplankton seston dominated by *Microcystis*	>100 μm	Cook et al., 2020 (24)
PRJNA386411	Lake Taihu, China, time series	Size-fractionated communities	>120 μm, 3–36 μm, 0.2–3 μm	Shi et al., 2018 (28)
PRJNA591360	Transects across the Laurentian Great Lakes in spring and summer	Free-living communities	0.22–1.6 μm	Paver et al., 2020 (124)
PRJNA479553	Monthly sampling of Nakdong River, South Korea	Whole water communities	>0.22 μm	Chun et al., 2019 (128)
PRJNA255432	Transect across the Laurentian Great Lakes	Whole water communities	>0.22 μm	Rozmarynowycz et al., 2019 (125)
PRJNA353865	Lake Champlain, Canada, time series	Whole water communities	>0.22 μm	Tromas et al., 2017 (127)
PRJEB14911	Lake Mendota, USA, time series	Whole water communities	>0.22 μm	Kara et al., 2013 (126)

teria CoA2 C42 or *Bryobacter* (Fig. S13). In other freshwater systems, there was also a significant positive correlation between *Bryobacter* relative abundance and *Microcystis* relative abundance (Fig. 5C). In contrast, acidobacterium CoA2 C42 had a significant negative correlation in other data sets, but the correlation was weak (Fig. 5D). The regression results indicate that strains related to both *Acidobacteria* species also occur in freshwater systems at times and locations where *Microcystis* is absent. However, in samples where *Microcystis* relative abundance was below 1%, *Bryobacter* relative abundance was typically lower (mean 0.001%), indicating that the highest *Bryobacter* relative abundance usually occurs during *Microcystis* blooms. Both *Acidobacteria* could also be absent while *Microcystis* was present at high abundance, suggesting that while both may occur in *Microcystis* blooms, they are not consistently present in all microbial communities associated with *Microcystis* blooms. An inconsistent cooccurrence between *Bryobacter* spp. and *Microcystis* is consistent with bacterial interactions with *Microcystis* being strain specific (27, 29, 37) and with uneven spatial and temporal distribution of *Microcystis* strains (95).

We assessed the abundance of both *Acidobacteria* groups in particle-attached microbial communities of various sizes, which may indicate physical association with phytoplankton, including *Microcystis*, which grow in large, buoyant colonies (96). The relative abundance of both *Bryobacter* and *Acidobacteria* CoA2 C42 amplicons was enriched in particle-attached communities (>100-μm retentate samples) during the 2014 western Lake Erie *Microcystis* bloom (Fig. 6). Similarly, although it was present in only August and September, *Bryobacter* was associated with the size fraction that contained the most *Microcystis* phytoplankton in Lake Taihu but was absent from smaller particles and free-living communities (Fig. 7). In contrast, acidobacterium CoA2 C42 was absent from large, *Microcystis*-containing aggregates and present in smaller particles and free-living communities in Lake Taihu (Fig. 7). *Bryobacter* was also absent from free-living communities throughout the Great Lakes, while acidobacterium CoA2 C42 was present (Fig. S14). A previous study identified *Bryobacter* in ~25% of *Microcystis* colonies sampled, while other *Acidobacteria* were largely absent (27), and another study found that *Bryobacter* relative abundance was significantly correlated with the relative abundance of certain *Microcystis* genotypes (37). Together with the relationships between *Acidobacteria* relative abundance and *Microcystis* relative abundance (Fig. 5), the relative abundance of *Bryobacter* in size-fractionated communities suggests that *Bryobacter* is present in some *Microcystis* blooms when conditions are favorable and physically attaches to *Microcystis* colonies, while acidobacterium CoA2 C42 likely facultatively colonizes other particles and is not specifically associated with *Microcystis* blooms.

Conclusions. This study reported insights into two novel, uncultured *Acidobacteria* species that are associated with phytoplankton seston in *Microcystis* blooms around the world. While both organisms were detected in *Microcystis* blooms, only *Bryobacter* was found directly associated with *Microcystis* colonies. The transcriptomic evidence

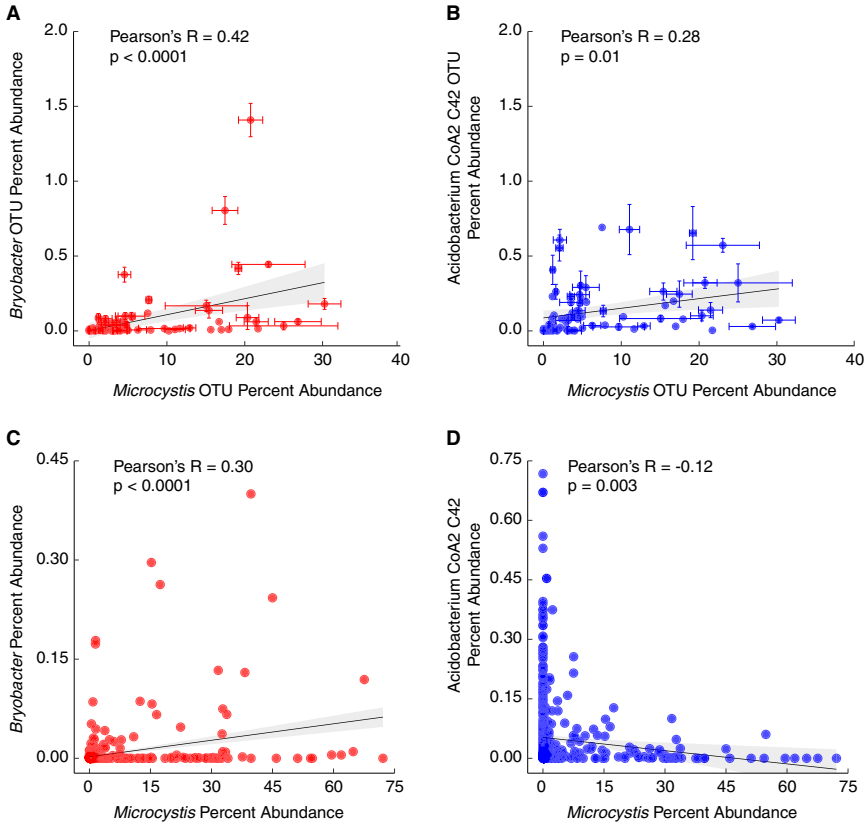

FIG 5 Percent abundance of *Bryobacter* and acidobacterium CoA2 C42 as a function of *Microcystis* percent abundance in whole water microbial community rRNA amplicon data sets from freshwaters. (A) *Bryobacter* OTU percent abundance versus *Microcystis* OTU percent abundance in V4 16S rRNA amplicon data sets collected during western Lake Erie cyanobacterial blooms. (B) acidobacterium CoA2 C42 OTU percent abundance versus *Microcystis* OTU percent abundance in V4 16S rRNA amplicon data sets collected during western Lake Erie cyanobacterial blooms. (C) The percent abundance of reads in published amplicon data sets that mapped to the 16S rRNA gene from the *Bryobacter* CoA8 C33 MAG versus the percent abundance of amplicon reads that mapped to 16S rRNA from *Microcystis*. (D) The percent abundance of reads in published amplicon data sets that mapped to the 16S rRNA gene from the acidobacterium CoA2 C42 MAG versus the percent abundance of amplicon reads that mapped to 16S rRNA from *Microcystis*. In all panels, the shaded area around the regression line indicates the regression standard error, error bars show the 95% confidence intervals determined from replicate filters (n = 4 or 8), and P values show the significance of the regression slope calculated with an F-test.

supports the hypothesis that *Bryobacter* and acidobacterium CoA2 C42 use organic carbon and nitrogen from dissolved organic matter present in phytoplankton lysate or exudate and regenerate reduced N that may fuel growth of other microorganisms, including *Microcystis*, which can grow using reduced N (30, 97, 98). The data also suggest that both *Acidobacteria* use cobalamins released into the environment by other organisms, which may include *Microcystis*. The inferred reciprocal exchange of metabolites between *Acidobacteria* and phytoplankton suggests potential for a mutualistic relationship, but additional work is required to test this hypothesis.

MATERIALS AND METHODS

DNA and RNA extraction and sequencing. Water samples were collected through the summer and fall of 2014 in western Lake Erie in order to monitor microbial communities and water chemistry throughout various stages of *Microcystis* bloom development (see references 36, 38, and 39 and Data Set S1 in the supplemental material for more detail about how the samples correspond to different times of year and *Microcystis* bloom development). Microbial samples were obtained from a 20-L depth-integrated water sample collected from the surface to 1 m above the lake bottom. Depth-integration was performed by collecting water with a peristaltic pump and slowly moving the length of the peristaltic pump tubing repeatedly up and down the water column until a 20-L carboy was filled completely. The integrated water column sampling method is critical to capture

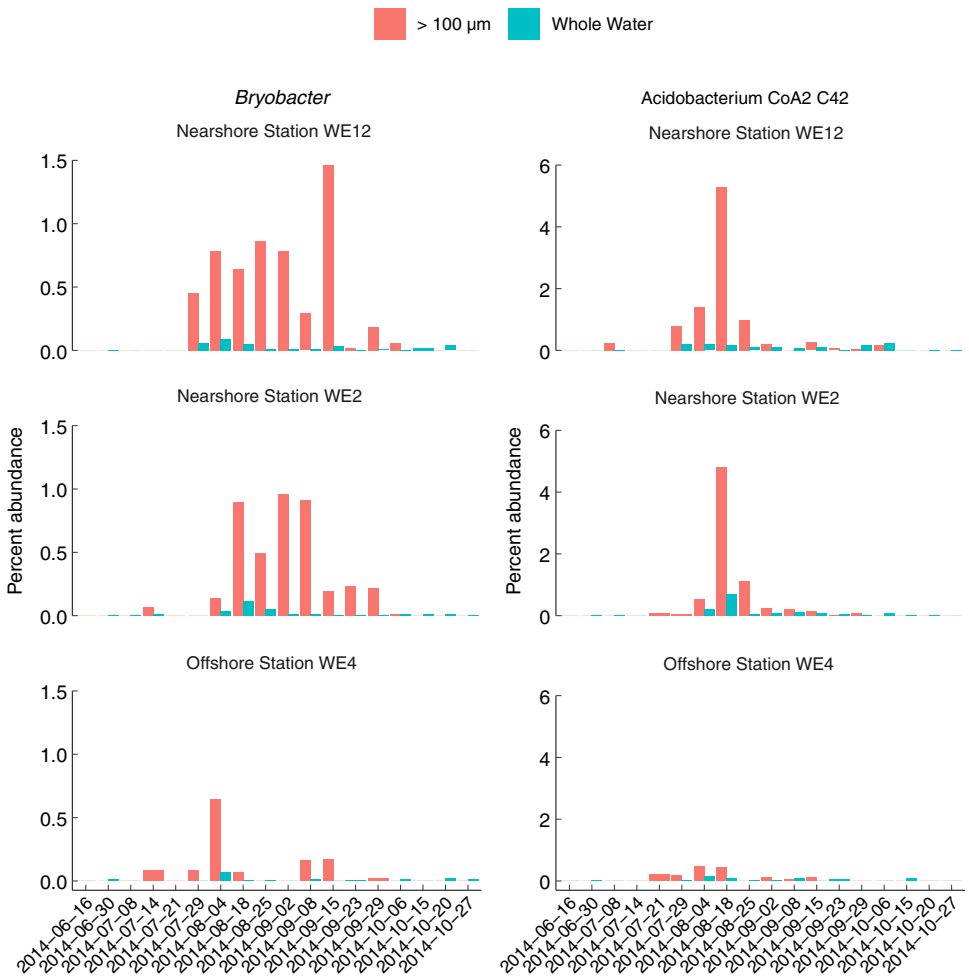

FIG 6 Percent abundance of *Bryobacter* and acidobacterium CoA2 C42 OTUs in size-fractionated samples from a western Lake Erie time series collected in the summer-fall of 2014. Bar colors depict size fraction.

the full bloom community because *Microcystis* cells can migrate vertically throughout the water column (96, 99).

To focus on the *Microcystis* colony-associated fraction, 2 L of depth-integrated sample was filtered through a 100-μm-pore-size mesh, and the retentate was backwashed into a Falcon tube using altered BG-11 medium (Table S1). RNAlater was added in a 2:1 ratio with the backwash, which was then filtered onto a 1.6-μm-pore-size glass fiber filter with a syringe. The backwash was filtered onto the 1.6-μm filter immediately after resuspension in BG-11 medium, so there was likely little or no effect of BG-11 on microbial community composition. The filters were stored in a 2-mL cryovial with 1 mL of RNAlater and kept on ice during cruise transit. Upon arrival at the lab, the filters were frozen at −80°C until extraction. We cannot rule out the possibility that free-living bacteria adhered to particles or that particle-attached bacteria were flushed from particles during sample collection. However, previous work using western Lake Erie samples collected with the same methods showed that >100-μm particle-associated communities were often distinct from whole water communities and that the degree of similarity was correlated with *Microcystis* abundance (27). Therefore, attached microbial communities are distinct from free-living communities collected with these methods, and any similarity between >100-μm particle-associated and whole water samples is likely due to a high abundance of *Microcystis* colonies in the water column at the time of sampling rather than capture of free-living bacteria by particles retained during filtration.

Filters with collected biomass were thawed, folded with biomass facing inward, and rinsed with sterile phosphate-buffered saline (PBS) to remove RNAlater preservative. Filters were incubated in 100 μL Qiagen ATL tissue lysis buffer, 300 μL Qiagen AL lysis buffer, and 30 μL proteinase K for 1 h at 56°C on a rotisserie (Qiagen, Hilden, Germany). Cells were further lysed by vortexing in this lysis buffer for 10 min. Lysates were homogenized using a QIAshredder column, and DNA was purified from the filtrate using the Qiagen DNeasy blood and tissue kit according to the manufacturer's standard protocol. The quantity and quality of DNA in each sample were determined using a NanoDrop Lite spectrophotometer (Thermo Scientific). DNA extracts were frozen at −80°C until analysis.

For RNA extraction, the filters were incubated in 600 μL Qiagen RLT+ buffer and 6 μL β-mercaptoethanol for 90 min on a rotisserie. The filters were then vortexed for 10 min and homogenized using a

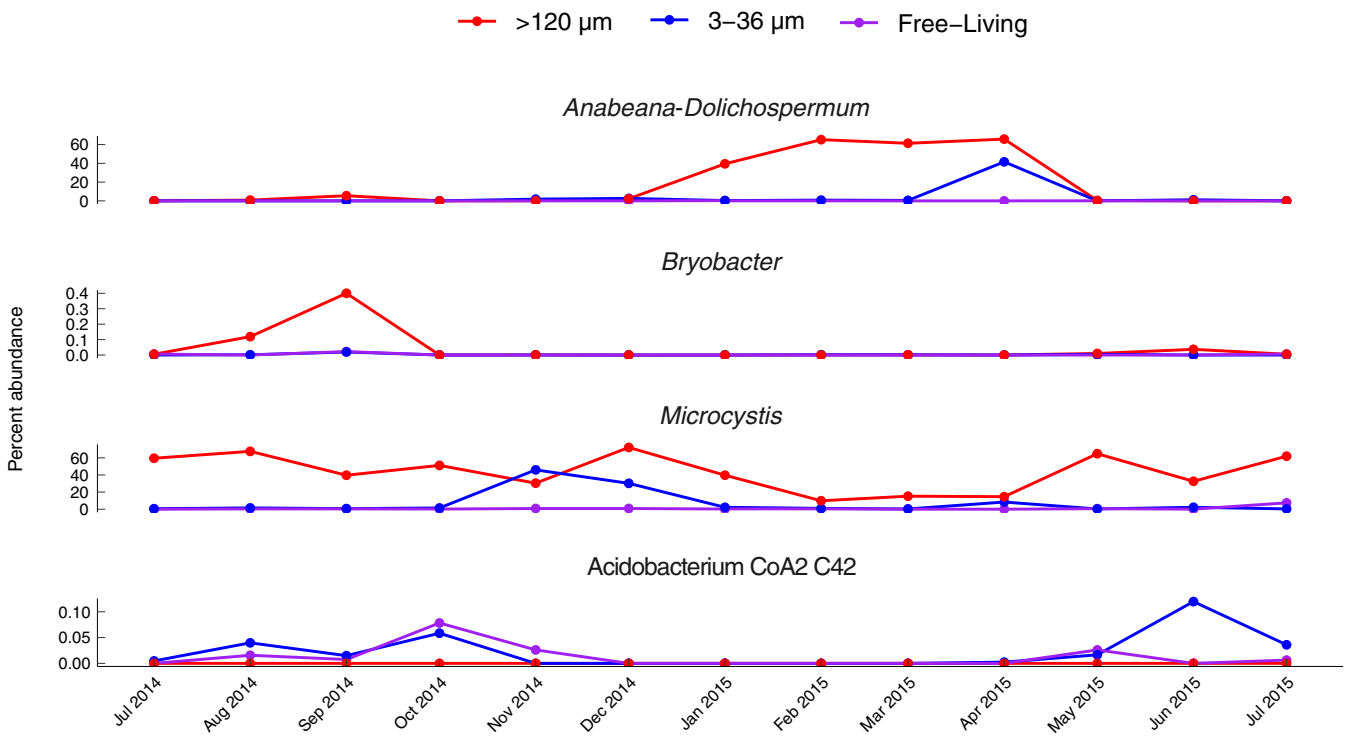

FIG 7 Percent abundance of *Acidobacteria* of interest and major *Cyanobacteria* taxa, *Anabaena-Dolichospermum* and *Microcystis*, in size-fractionated samples from a time series of Lake Taihu cyanobacterial blooms.

QIAshredder column. RNA was purified from the homogenized solution using the RNeasy kit according to the manufacturer's standard protocol.

All sequencing was performed at the University of Michigan Sequencing Core. Paired-end DNA sequencing (2 × 125) was conducted on an Illumina HiSeq 2000 with V4 chemistry reagents with "low-input prep" using the Rubicon ThruPlex kit. RNA single-read sequencing (1 × 50) was performed on an Illumina HiSeq 2000 with V4 chemistry reagents. Before sequencing, RNA libraries were prepared with a 50/50 mix of plant and bacterial Ribo-Zero kits to remove rRNA sequences.

Metagenomic assembly. Combined-sample assemblies (coassemblies) were generated with MEGAHIT (100) using kmin 21, kmax 141, and kmer step size of 12. We performed 3 coassemblies in total, choosing samples based on the abundance of the target *Acidobacteria* organisms estimated from 16S rRNA gene amplicon sequences. One coassembly was generated with the only two samples that yielded low-quality *Acidobacteria* genomes in pilot single-sample assemblies (Aug-4 and Aug-25 particle metagenomes from WE12). Another coassembly was constructed with all the samples in which *Acidobacteria* CoA2 C42 was present in corresponding amplicon sequence data sets (8 samples total), and another with the same 8 samples but with the read kmer coverage normalized to 20× prior to assembly with BBnorm in the BBTools package (101). Paired-end reads were quality and adapter screened and dereplicated with BBTools prior to coassembly (101). An additional single-sample MEGAHIT assembly was constructed on the particle size fraction sample from 4 August at WE12 following the same pipeline. This sample was chosen for assembly because it represented peak particulate microcystin (cyanotoxin) concentrations for this location (102), which is of particular societal importance because it is near the drinking water intake for Toledo, OH, a city that lost access to drinking water due to cyanotoxins in August during the year of sampling (103).

Genome binning. Contigs were binned using a multialgorithm binning approach. Contigs were binned using differential coverage and tetranucleotide frequencies in CONCOCT (104) and Metabat2 (105) and with tetranucleotide frequencies alone using VizBin (106) and Emergent Self-Organizing Maps (ESOMs) (107). The contig size window for ESOM was 4 to 10 kbp and 2.5 to 10 kbp for the other binners. The resulting redundant bin data sets from each assembly were dereplicated using DASTool (108). For the single-sample assembly, differential coverage was estimated by mapping reads from 4 August WE12 and 25 August WE12 to the contigs. For coassemblies, differential coverage was estimated by mapping reads from the corresponding samples used to generate the coassemblies. Read mapping to contigs was performed using Bowtie2 (109).

The bins were refined manually in Anvi'o (110) using contig coverage and ward linkage clustering of tetranucleotide frequencies. Quality metrics of the refined bins were estimated using the lineage workflow in CheckM (111). All bins with contamination scores greater than 5% after refinement were eliminated from downstream analysis. Contamination scores of the final bins were considered while ignoring the amount of contamination due to strain heterogeneity. Redundant marker genes were considered to be from closely related strains if their shared amino acid identity was 95% or greater. This redundant bin

data set was dereplicated using dRep (112) with 97% ANI and 60% alignment coverage cutoffs and skipping the MASH preclustering step. The final bin for the acidobacterium CoA2 C42 genome came from the 2-sample coassembly, and the final bin for the *Bryobacter* CoA8 C33 genome came from the 8-sample coassembly without kmer normalization.

Gene annotation and metatranscriptomic read mapping. Gene calls and functional annotations were generated using the Integrated Microbial Genomes annotation pipeline (113), and membrane-associated proteins were predicted using TransportDB v. 2.0 (114). Genes annotated as iron complex transporters were compared to biochemically confirmed cobalamin transporters from *Escherichia coli* strain K-12 (UniProtKB accession numbers: P06129, P06609, and P06611) via protein BLAST v. 2.2.31+ (115). We excluded any significant hits in the results with alignment coverage less than 70% of the gene in the *Acidobacteria* genomes.

All predicted open reading frames were compared to proteins in the NCBI nonredundant protein database (as of 17 October 2018) via protein BLAST v. 2.2.31+ (115). Gene expression was determined by mapping metatranscriptomic reads to predicted gene sequences using nucleotide BLAST v. 2.2.31+ (115). Only alignments with percent identity of ≥95%, E value of $\leq 1 \times 10^{-5}$, and alignment coverage of ≥80% of read length were counted. Some reads below the alignment coverage cutoff were counted if they mapped to either the start or stop end of the gene. The relative abundance of transcripts for each gene was calculated as reads mapped per gene kilobase per million reads mapped (RPKM), using total number of reads mapped to the appropriate genome. Reads were competitively mapped to both *Acidobacteria* MAGs and the following *Microcystis* reference genomes: *Microcystis* strain FD4, strain NIES 843, strain NIES 2481, strain NIES 2549, and strain PCC 7806SL.

Predicted gene calls, functional annotations, and metatranscriptomic gene mapping were used to infer *in situ* metabolism of *Bryobacter* and acidobacterium CoA2 C42. Due to the novelty of the *Acidobacteria* genomes reported here, most of the predicted protein-coding genes have low shared amino acid identities with published protein sequences with the same function (<70% shared identity to the best matches in many cases [Fig. S1]), so we present these results as putative functions and interactions of interest that require validation with future work. Because acidobacterium CoA2 C42 had a sufficient amount of reads only in the 4 August sample (Fig. S2), which coincided with an early peak in phytoplankton pigments at this station (102), this sample was the focus of reported RPKM values in the main text and figures.

16S rRNA gene phylogenetic and gANI analyses. The 16S rRNA genes from each MAG were compared to the SILVA SSU database v. 138.1 (116) using the online SINA Aligner v. 1.2.11 (117) and classified using the approach of Wang et al. (118) in MOTHUR v. 1.43.0 (119). One MAG (CoA2 C42) was not binned with an rRNA operon, but an unbinned contig with the full rRNA operon was assigned to the bin by examining the assembly De Bruijn graph using Bandage v. 0.8.1 (120) and the paired-end mapping information. A maximum likelihood phylogenetic tree with published 16S rRNA genes from *Acidobacteria* available in NCBI (as of 8 November 2020) was computed with RAxML v. 8.2.4 using the GTRGAMMA nucleotide substitution model (121) and rooted and visualized using the Interactive Tree of Life webtool v 6.3 (122). The 16S rRNA genes were aligned using Clustal Omega v. 1.2.1 (123). Shared average nucleotide identity (gANI) was computed with whole-genome alignments of *Acidobacteria* genomes available in IMG (as of 5 November 2018) using the compare function in dRep v. 2.0.5 (112) without the MASH preclustering step. Genomes were included in the gANI analysis only if the completeness and the contamination calculated with the CheckM lineage workflow were above 90% and below 5%, respectively (111).

Amplicon data set mining. To assess the frequency of occurrence of the *Acidobacteria* in *Microcystis* blooms, we searched for their presence in previously published rRNA amplicon data sets (24, 28, 102, 124–128), which are described in Table 3. To assess the MAGs' abundance in western Lake Erie, the relative abundances of operational taxonomic units (OTUs) from a previously published abundance matrix were reported (27). For the *Bryobacter* CoA8 C33 MAG, the relative abundance of OTUs classified as *Bryobacter* was reported. For the acidobacterium CoA2 C42 MAG, the relative abundance of OTUs classified as *Paludibaculum* was reported if the 16S rRNA gene in the MAG aligned with the amplicon sequence with 97% or more shared nucleotide identity as determined via nucleotide BLAST v. 2.2.31+ (115).

Because other data sets used a range of different primer sets and did not provide abundance tables, we determined the abundance of each organism in these data sets by mapping amplicon reads to the 16S rRNA gene sequence in each MAG with BLAST v. 2.2.31+ (115). The relative abundances of *Microcystis*, *Synechococcus*, and *Dolichospermum* were similarly determined in these data sets by mapping amplicon reads to reference sequences. We mapped to full-length 16S rRNA gene sequences from *Anabaena cylindrica* PCC 7122, *Microcystis aeruginosa* PCC 7806SL, *Microcystis aeruginosa* PCC 9806, *Synechococcus elongatus* PCC 6301, and *Synechococcus elongatus* PCC 7942, as well as sequences assembled from Lake Erie metagenomes using EMIRGE (129) and classified as *Microcystis*, *Anabaena*, *Dolichospermum*, and *Synechococcus* using the classifier of Wang et al. (118) in MOTHUR v 1.43.0 (119). The relative abundance of each organism in each sample was calculated as the number of reads mapped for that given organism divided by the total number of reads in the data set.

Identification of pseudocobalamin in *Microcystis* cultures. Two strains of *Microcystis aeruginosa* (PCC 7806 and PCC 9806) were grown on modified BG-11 growth medium (130) with the sodium nitrate concentration reduced to 2 mM in preparation for screening for pseudocobalamin production via liquid chromatography-mass spectrometry (LC-MS) analysis. The *Microcystis* strains were grown as batch cultures at room temperature under cool white fluorescent bulbs. The light intensity was kept between 30 and 60 μmol photons/m^2/s by covering the lights with a single layer of neutral-density 0.3 filter screen (product 209R; Lee Filters, Burbank, CA). For each strain, 300 mL of late-log-phase culture was split into six 50-mL aliquots and harvested by centrifugation at 10,000 × *g* for 15 min, decanting liquid media, and freezing at −80°C until extraction.

Analysis of cell pellets was carried out using a previously published method (8), with some modifications. Briefly, cell pellets were resuspended in 6 mL of cold acetonitrile-methanol-water (40:40:20 ratio

by volume) with 0.1% formic acid and transferred to 15-mL centrifuge tubes. The cells were lysed via bead beating with 250 mg each of 100- and 500-μm-diameter glass beads on a vortex mixer set to maximum speed for 40 s. Bead beating was performed three times, with samples resting on ice for 5 min between each treatment. The suspension was pelleted via centrifugation at 10,000 $\times$ *g*, and the supernatant was transferred to a round-bottom flask. The pooled supernatants from each strain were dried in a rotary evaporator under pressure of 0.3 $\times$ 10^5 Pa at 30°C and then resuspended in a small volume of solvent A (described below) before LC-MS analysis. Extraction from ~6 g *Spirulina* powder was also performed as a positive control (8) following the same procedure described above for the *Microcystis* cells, with the exception that the powder was suspended in 10 mL of cold acetonitrile-methanol-water solution (40:40:20 ratio by volume). All extraction and processing steps were conducted under low-light conditions to minimize photodegradation of pseudocobalamin.

LC-MS analysis was carried out on a Thermo Scientific ultrahigh-pressure liquid chromatograph (UHPLC) coupled to a Q-Exactive Orbitrap high-resolution mass spectrometer equipped with an electrospray ionization (ESI) source and running in positive mode. Sample (5 μL) was injected onto a 2.6-μm Kinetex RP C_{18} column (150- by 4.6-mm inside diameter) held at 25°C. The HPLC gradient used was 5% to 95% solvent B over 22 min, where solvent A consisted of 20 mM ammonium formate and 0.1% formic acid in water, and solvent B consisted of 0.1% formic acid in acetonitrile. MS data were collected over a mass range of 600 to 1,400 *m/z*, using data-dependent MS/MS analysis with 0.5-s dynamic exclusion enabled. Pseudocobalamin variants were identified by comparing the obtained compound masses and MS/MS spectra to previously reported literature values (8, 131) and the *Spirulina* extract.

Scripts and data availability. All data tables and shell and R code used for the analysis are included on GitHub at the following web address: https://github.com/Geo-omics/WLE-Acidobacteria-Genomes. Acidobacterial MAG sequences and gene annotations are deposited and publicly available in the IMG database (IMG genome IDs: 2806310633 and 2806310632). Assembled MAG sequences are also available in NCBI (BioSample accession numbers SAMN20863144 and SAMN20863205). Raw read data sets are publicly available in NCBI SRA under BioSample accession numbers SAMN09102072 to SAMN09102087, and Whole Genome Shotgun projects have been deposited at DDBJ/ENA/GenBank under the accession numbers JAINDK000000000 and JAINDL000000000. Full metagenome assemblies from which the MAGs were derived are publicly available in IMG (IMG genome IDs: 3300028429 and 3300028430). Raw metabolomic data are submitted to the GNPS-MassIVE database under the following ID: MassIVE MSV000088058. Accession numbers are listed for each sample and assembly in Data Set S1 in the supplemental material.

SUPPLEMENTAL MATERIAL

Supplemental material is available online only.

SUPPLEMENTAL FILE 1, PDF file, 1.9 MB.

SUPPLEMENTAL FILE 2, XLSX file, 0.03 MB.

SUPPLEMENTAL FILE 3, XLSX file, 1.5 MB.

SUPPLEMENTAL FILE 4, XLSX file, 1.7 MB.

SUPPLEMENTAL FILE 5, XLSX file, 0.01 MB.

ACKNOWLEDGMENTS

We thank Robert Hein for bioinformatics and computational support, Rose Cory, Tim Davis, and George Kling for feedback on initial drafts of the manuscript, and the Cooperative Institute for Great Lakes Research and NOAA Great Lakes Environmental Laboratory for assistance with field work and sample collection.

This work was supported by the National Science Foundation grant OCE-1736629, the Rackham Graduate School at the University of Michigan, and the Biological Sciences Scholar Program at the University of Michigan (R.D.K.). Part of this work was funded by Lawrence Livermore National Laboratory's Laboratory Directed Research and Development grant 20-ERD-061. Lawrence Livermore National Laboratory is operated by Lawrence Livermore National Security, LLC, for the U.S. Department of Energy, National Nuclear Security Administration, under contract DE-AC52-07NA27344.

We have no conflicts of interest to report.

REFERENCES

1. Anantharaman K, Brown CT, Hug LA, Sharon I, Castelle CJ, Probst AJ, Thomas BC, Singh A, Wilkins MJ, Karaoz U, Brodie EL, Williams KH, Hubbard SS, Banfield JF. 2016. Thousands of microbial genomes shed light on interconnected biogeochemical processes in an aquifer system. Nat Commun 7:13219. https://doi.org/10.1038/ncomms13219.
2. Embree M, Liu JK, Al-Bassam MM, Zengler K. 2015. Networks of energetic and metabolic interactions define dynamics in microbial communities. Proc Natl Acad Sci U S A 112:15450–15455. https://doi.org/10.1073/pnas.1506034112.
3. Hug LA, Co R. 2018. It takes a village: microbial communities thrive through interactions and metabolic handoffs. mSystems 3:e00152-17. https://doi.org/10.1128/mSystems.00152-17.
4. Durham BP, Dearth SP, Sharma S, Amin SA, Smith CB, Campagna SR, Armbrust EV, Moran MA. 2017. Recognition cascade and metabolite transfer

in a marine bacteria-phytoplankton model system. Environ Microbiol 19:3500–3513. https://doi.org/10.1111/1462-2920.13834.
5. Durham BP, Sharma S, Luo H, Smith CB, Amin SA, Bender SJ, Dearth SP, Van Mooy BAS, Campagna SR, Kujawinski EB, Armbrust EV, Moran MA. 2015. Cryptic carbon and sulfur cycling between surface ocean plankton. Proc Natl Acad Sci U S A 112:453–457. https://doi.org/10.1073/pnas.1413137112.
6. Ma AT, Tyrell B, Beld J. 2020. Specificity of cobamide remodeling, uptake, and utilization in *Vibrio cholerae*. Mol Microbiol 113:89–102. https://doi.org/10.1111/mmi.14402.
7. Gray MJ, Escalante-Semerena JC. 2009. The cobinamide amidohydrolase (cobyric acid-forming) CbiZ enzyme: a critical activity of the cobamide remodelling system of *Rhodobacter sphaeroides*. Mol Microbiol 74:1198–1210. https://doi.org/10.1111/j.1365-2958.2009.06928.x.
8. Heal KR, Qin W, Ribalet F, Bertagnolli AD, Coyote-Maestas W, Hmelo LR, Moffett JW, Devol AH, Armbrust EV, Stahl DA, Ingalls AE. 2017. Two distinct pools of B12 analogs reveal community interdependencies in the ocean. Proc Natl Acad Sci U S A 114:364–369. https://doi.org/10.1073/pnas.1608462114.
9. Croft MT, Lawrence AD, Raux-Deery E, Warren MJ, Smith AG. 2005. Algae acquire vitamin B_{12} through a symbiotic relationship with bacteria. Nature 438:90–93. https://doi.org/10.1038/nature04056.
10. Amin SA, Green DH, Hart MC, Küpper FC, Sunda WG, Carrano CJ. 2009. Photolysis of iron-siderophore chelates promotes bacterial-algal mutualism. Proc Natl Acad Sci U S A 106:17071–17076. https://doi.org/10.1073/pnas.0905512106.
11. Amin SA, Hmelo LR, van Tol HM, Durham BP, Carlson LT, Heal KR, Morales RL, Berthiaume CT, Parker MS, Djunaedi B, Ingalls AE, Parsek MR, Moran MA, Armbrust EV. 2015. Interaction and signalling between a cosmopolitan phytoplankton and associated bacteria. Nature 522:98–101. https://doi.org/10.1038/nature14488.
12. Arandia-Gorostidi N, Weber PK, Alonso-Sáez L, Morán XAG, Mayali X. 2017. Elevated temperature increases carbon and nitrogen fluxes between phytoplankton and heterotrophic bacteria through physical attachment. ISME J 11:641–650. https://doi.org/10.1038/ismej.2016.156.
13. Christie-Oleza JA, Sousoni D, Lloyd M, Armengaud J, Scanlan DJ. 2017. Nutrient recycling facilitates long-term stability of marine microbial phototroph-heterotroph interactions. Nat Microbiol 2:17100. https://doi.org/10.1038/nmicrobiol.2017.100.
14. Morris JJ, Johnson ZI, Szul MJ, Keller M, Zinser ER. 2011. Dependence of the cyanobacterium *Prochlorococcus* on hydrogen peroxide scavenging microbes for growth at the ocean's surface. PLoS One 6:e16805. https://doi.org/10.1371/journal.pone.0016805.
15. Segev E, Wyche TP, Kim KH, Petersen J, Ellebrandt C, Vlamakis H, Barteneva N, Paulson JN, Chai L, Clardy J, Kolter R. 2016. Dynamic metabolic exchange governs a marine algal-bacterial interaction. Elife 5:e17473. https://doi.org/10.7554/eLife.17473.
16. Seyedsayamdost MR, Case RJ, Kolter R, Clardy J. 2011. The Jekyll-and-Hyde chemistry of *Phaeobacter gallaeciensis*. Nat Chem 3:331–335. https://doi.org/10.1038/nchem.1002.
17. Bell W, Mitchell R. 1972. Chemotactic and growth responses of marine bacteria to algal extracellular products. Biol Bull 143:265–277. https://doi.org/10.2307/1540052.
18. Seymour JR, Amin SA, Raina J-B, Stocker R. 2017. Zooming in on the phycosphere: the ecological interface for phytoplankton-bacteria interactions. Nat Microbiol 2:17065. https://doi.org/10.1038/nmicrobiol.2017.65.
19. Schmidt KC, Jackrel SL, Smith DJ, Dick GJ, Denef VJ. 2020. Genotype and host microbiome alter competitive interactions between *Microcystis aeruginosa* and *Chlorella sorokiniana*. Harmful Algae 99:101939. https://doi.org/10.1016/j.hal.2020.101939.
20. Cole JJ. 1982. Interactions between bacteria and algae in aquatic ecosystems. Annu Rev Ecol Syst 13:291–314. https://doi.org/10.1146/annurev.es.13.110182.001451.
21. Smriga S, Fernandez VI, Mitchell JG, Stocker R. 2016. Chemotaxis toward phytoplankton drives organic matter partitioning among marine bacteria. Proc Natl Acad Sci U S A 113:1576–1581. https://doi.org/10.1073/pnas.1512307113.
22. Sison-Mangus MP, Jiang S, Tran KN, Kudela RM. 2014. Host-specific adaptation governs the interaction of the marine diatom, *Pseudo-nitzschia* and their microbiota. ISME J 8:63–76. https://doi.org/10.1038/ismej.2013.138.
23. Harke MJ, Steffen MM, Gobler CJ, Otten TG, Wilhelm SW, Wood SA, Paerl HW. 2016. A review of the global ecology, genomics, and biogeography of the toxic cyanobacterium, *Microcystis* spp. Harmful Algae 54:4–20. https://doi.org/10.1016/j.hal.2015.12.007.
24. Cook KV, Li C, Cai H, Krumholz LR, Hambright KD, Paerl HW, Steffen MM, Wilson AE, Burford MA, Grossart H-P, Hamilton DP, Jiang H, Sukenik A, Latour D, Meyer EI, Padisák J, Qin B, Zamor RM, Zhu G. 2020. The global *Microcystis* interactome. Limnol Oceanogr 65:S194–S207. https://doi.org/10.1002/lno.11361.
25. Wang K, Mou X. 2021. Coordinated diel gene expression of cyanobacteria and their microbiome. Microorganisms 9:1670. https://doi.org/10.3390/microorganisms9081670.
26. Parveen B, Ravet V, Djediat C, Mary I, Quiblier C, Debroas D, Humbert JF. 2013. Bacterial communities associated with *Microcystis* colonies differ from free-living communities living in the same ecosystem. Environ Microbiol Rep 5:716–724. https://doi.org/10.1111/1758-2229.12071.
27. Smith DJ, Tan JY, Powers MA, Lin XN, Davis TW, Dick GJ. 2021. Individual *Microcystis* colonies harbor distinct bacterial communities that differ by *Microcystis* oligotype and with time. Environ Microbiol 23:3020–3036. https://doi.org/10.1111/1462-2920.15514.
28. Shi L, Huang Y, Zhang M, Shi X, Cai Y, Gao S, Tang X, Chen F, Lu Y, Kong F. 2018. Large buoyant particles dominated by cyanobacterial colonies harbor distinct bacterial communities from small suspended particles and free-living bacteria in the water column. Microbiologyopen 7:e00608. https://doi.org/10.1002/mbo3.608.
29. Pérez-Carrascal OM, Tromas N, Terrat Y, Moreno E, Giani A, Corrêa Braga Marques L, Fortin N, Shapiro BJ. 2021. Single-colony sequencing reveals microbe-by-microbiome phylosymbiosis between the cyanobacterium *Microcystis* and its associated bacteria. Microbiome 9:194. https://doi.org/10.1186/s40168-021-01140-8.
30. Davis TW, Harke MJ, Marcoval MA, Goleski J, Orano-Dawson C, Berry DL, Gobler CJ. 2010. Effects of nitrogenous compounds and phosphorus on the growth of toxic and non-toxic strains of *Microcystis* during cyanobacterial blooms. Aquat Microb Ecol 61:149–162. https://doi.org/10.3354/ame01445.
31. Kardinaal WEA, Janse I, Kamst-van Agterveld M, Meima M, Snoek J, Mur LR, Huisman J, Zwart G, Visser PM. 2007. *Microcystis* genotype succession in relation to microcystin concentrations in freshwater lakes. Aquat Microb Ecol 48:1–12. https://doi.org/10.3354/ame048001.
32. Shia L, Cai Y, Wang X, Li P, Yu Y, Kong F. 2010. Community structure of bacteria associated with *Microcystis* colonies from cyanobacterial blooms. J Freshw Ecol 25:193–203. https://doi.org/10.1080/02705060.2010.9665068.
33. Chen Z, Zhang J, Li R, Tian F, Shen Y, Xie X, Ge Q, Lu Z. 2018. Metatranscriptomics analysis of cyanobacterial aggregates during cyanobacterial bloom period in Lake Taihu, China. Environ Sci Pollut Res Int 25:4811–4825. https://doi.org/10.1007/s11356-017-0733-4.
34. Davenport EJ, Neudeck MJ, Matson PG, Bullerjahn GS, Davis TW, Wilhelm SW, Denney MK, Krausfeldt LE, Stough JMA, Meyer KA, Dick GJ, Johengen TH, Lindquist E, Tringe SG, McKay RML. 2019. Metatranscriptomic analyses of diel metabolic functions during a *Microcystis* bloom in western Lake Erie (United States). Front Microbiol 10:2081. https://doi.org/10.3389/fmicb.2019.02081.
35. Penn K, Wang J, Fernando SC, Thompson JR. 2014. Secondary metabolite gene expression and interplay of bacterial functions in a tropical freshwater cyanobacterial bloom. ISME J 8:1866–1878. https://doi.org/10.1038/ismej.2014.27.
36. Smith DJ, Berry MA, Cory RM, Johengen TJ, Kling GW, Davis TW, Dick GJ. 2022. Heterotrophic bacteria dominate catalase expression during *Microcystis* blooms. Appl Environ Microbiol 88:e2544-21.
37. Chun S-J, Cui Y, Lee JJ, Choi I-C, Oh H-M, Ahn C-Y. 2020. Network analysis reveals succession of Microcystis genotypes accompanying distinctive microbial modules with recurrent patterns. Water Res 170:115326. https://doi.org/10.1016/j.watres.2019.115326.
38. Berry MA, White JD, Davis TW, Jain S, Johengen TH, Dick GJ, Sarnelle O, Denef VJ. 2017. Are oligotypes meaningful ecological and phylogenetic units? A case study of *Microcystis* in freshwater lakes. Front Microbiol 8:365. https://doi.org/10.3389/fmicb.2017.00365.
39. Cory RM, Davis TW, Dick GJ, Johengen T, Denef VJ, Berry MA, Page SE, Watson SB, Yuhas K, Kling GW. 2016. Seasonal dynamics in dissolved organic matter, hydrogen peroxide, and cyanobacterial blooms in Lake Erie. Front Mar Sci 3:54.
40. Paerl HW, Otten TG. 2013. Blooms bite the hand that feeds them. Science 342:433–434. https://doi.org/10.1126/science.1245276.
41. Bowers RM, Kyrpides NC, Stepanauskas R, Harmon-Smith M, Doud D, Reddy TBK, Schulz F, Jarett J, Rivers AR, Eloe-Fadrosh EA, Tringe SG, Ivanova NN, Copeland A, Clum A, Becraft ED, Malmstrom RR, Birren B,

Podar M, Bork P, Weinstock GM, Garrity GM, Dodsworth JA, Yooseph S, Sutton G, Glöckner FO, Gilbert JA, Nelson WC, Hallam SJ, Jungbluth SP, Ettema TJG, Tighe S, Konstantinidis KT, Liu W-T, Baker BJ, Rattei T, Eisen JA, Hedlund B, McMahon KD, Fierer N, Knight R, Finn R, Cochrane G, Karsch-Mizrachi I, Tyson GW, Rinke C, Genome Standards Consortium, Lapidus A, Meyer F, Yilmaz P, Parks DH, Eren AM, Schriml L, Banfield JF, Hugenholtz P, Woyke T. 2017. Minimum information about a single amplified genome (MISAG) and a metagenome-assembled genome (MIMAG) of bacteria and archaea. Nat Biotechnol 35:725–731. https://doi.org/10.1038/nbt.3893.

42. Kulichevskaya IS, Suzina NE, Liesack W, Dedysh SN. 2010. *Bryobacter aggregatus* gen. nov., sp. nov., a peat-inhabiting, aerobic chemoorganotroph from subdivision 3 of the *Acidobacteria*. Int J Syst Evol Microbiol 60:301–306. https://doi.org/10.1099/ijs.0.013250-0.
43. Kulichevskaya IS, Suzina NE, Rijpstra WIC, Damste JSS, Dedysh SN. 2014. *Paludibaculum fermentans* gen. nov., sp. nov., a facultative anaerobe capable of dissimilatory iron reduction from subdivision 3 of the Acidobacteria. Int J Syst Evol Microbiol 64:2857–2864. https://doi.org/10.1099/ijs.0.066175-0.
44. Yarza P, Yilmaz P, Pruesse E, Glöckner FO, Ludwig W, Schleifer K-H, Whitman WB, Euzéby J, Amann R, Rosselló-Móra R. 2014. Uniting the classification of cultured and uncultured bacteria and archaea using 16S rRNA gene sequences. Nat Rev Microbiol 12:635–645. https://doi.org/10.1038/nrmicro3330.
45. Varghese NJ, Mukherjee S, Ivanova N, Konstantinidis KT, Mavrommatis K, Kyrpides NC, Pati A. 2015. Microbial species delineation using whole genome sequences. Nucleic Acids Res 43:6761–6771. https://doi.org/10.1093/nar/gkv657.
46. Konstantinidis KT, Tiedje JM. 2005. Genomic insights that advance the species definition for prokaryotes. Proc Natl Acad Sci U S A 102:2567–2572. https://doi.org/10.1073/pnas.0409727102.
47. Jones RT, Robeson MS, Lauber CL, Hamady M, Knight R, Fierer N. 2009. A comprehensive survey of soil acidobacterial diversity using pyrosequencing and clone library analyses. ISME J 3:442–453. https://doi.org/10.1038/ismej.2008.127.
48. Serkebaeva YM, Kim Y, Liesack W, Dedysh SN. 2013. Pyrosequencing-based assessment of the bacteria diversity in surface and subsurface peat layers of a northern wetland, with focus on poorly studied phyla and candidate divisions. PLoS One 8:e63994. https://doi.org/10.1371/journal.pone.0063994.
49. Robbins SJ, Song W, Engelberts JP, Glasl B, Slaby BM, Boyd J, Marangon E, Botté ES, Laffy P, Thomas T, Webster NS. 2021. A genomic view of the microbiome of coral reef demosponges. ISME J 15:1641–1654. https://doi.org/10.1038/s41396-020-00876-9.
50. Quaiser A, López-García P, Zivanovic Y, Henn MR, Rodriguez-Valera F, Moreira D. 2008. Comparative analysis of genome fragments of Acidobacteria from deep Mediterranean plankton. Environ Microbiol 10:2704–2717. https://doi.org/10.1111/j.1462-2920.2008.01691.x.
51. Dedysh SN, Sinninghe Damsté JS. 2018. Acidobacteria, p 1–10. *In* eLS. John Wiley & Sons, Ltd, Chichester, United Kingdom.
52. Wolk CP. 1973. Physiology and cytological chemistry blue-green algae. Bacteriol Rev 37:32–101. https://doi.org/10.1128/br.37.1.32-101.1973.
53. Plude JL, Parker DL, Schommer OJ, Timmerman RJ, Hagstrom SA, Joers JM, Hnasko R. 1991. Chemical characterization of polysaccharide from the slime layer of the cyanobacterium *Microcystis flos-aquae* C3-40. Appl Environ Microbiol 57:1696–1700. https://doi.org/10.1128/aem.57.6.1696-1700.1991.
54. Forni C, Telo' FR, Caiola MG. 1997. Comparative analysis of the polysaccharides produced by different species of *Microcystis* (Chroococcales, Cyanophyta). Phycologia 36:181–185. https://doi.org/10.2216/i0031-8884-36-3-181.1.
55. Li P, Cai Y, Shi L, Geng L, Xing P, Yu Y, Kong F, Wang Y. 2009. Microbial degradation and preliminary chemical characterization of *Microcystis* exopolysaccharides from a cyanobacterial water bloom of Lake Taihu. Int Rev Hydrobiol 94:645–655. https://doi.org/10.1002/iroh.200911149.
56. Grossart H-P, Simon M. 2007. Interactions of planktonic algae and bacteria: effects on algal growth and organic matter dynamics. Aquat Microb Ecol 47:163–176. https://doi.org/10.3354/ame047163.
57. Meon B, Kirchman DL. 2001. Dynamics and molecular composition of dissolved organic material during experimental phytoplankton blooms. Mar Chem 75:185–199. https://doi.org/10.1016/S0304-4203(01)00036-6.
58. Mühlenbruch M, Grossart HP, Eigemann F, Voss M. 2018. Mini-review: phytoplankton-derived polysaccharides in the marine environment and their interactions with heterotrophic bacteria. Environ Microbiol 20:2671–2685. https://doi.org/10.1111/1462-2920.14302.
59. Ferrer-González FX, Widner B, Holderman NR, Glushka J, Edison AS, Kujawinski EB, Moran MA. 2021. Resource partitioning of phytoplankton metabolites that support bacterial heterotrophy. ISME J 15:762–773. https://doi.org/10.1038/s41396-020-00811-y.
60. Kirchman DL, Keil RG, Wheeler PA. 1989. The effect of amino acids on ammonium utilization and regeneration by heterotrophic bacteria in the subarctic Pacific. Deep Sea Res I Oceanogr Res Pap 36:1763–1776. https://doi.org/10.1016/0198-0149(89)90071-X.
61. Tupas L, Koike I. 1990. Amino acid and ammonium utilization by heterotrophic marine bacteria grown in enriched seawater. Limnol Oceanogr 35:1145–1155. https://doi.org/10.4319/lo.1990.35.5.1145.
62. Tupas LM, Koike I, Karl DM, Holm-Hansen O. 1994. Nitrogen metabolism by heterotrophic bacterial assemblages in Antarctic coastal waters. Polar Biol 14:195–204. https://doi.org/10.1007/BF00240524.
63. Beliaev AS, Romine MF, Serres M, Bernstein HC, Linggi BE, Markillie LM, Isern NG, Chrisler WB, Kucek LA, Hill EA, Pinchuk GE, Bryant DA, Wiley HS, Fredrickson JK, Konopka A. 2014. Inference of interactions in cyanobacterial-heterotrophic co-cultures via transcriptome sequencing. ISME J 8:2243–2255. https://doi.org/10.1038/ismej.2014.69.
64. Palenik B, Morel FM. 1990. Comparison of cell-surface L-amino acid oxidases from several marine phytoplankton. Mar Ecol Prog Ser 59:195–201. https://doi.org/10.3354/meps059195.
65. Palenik B, Morel FM. 1990. Amino acid utilization by marine phytoplankton: a novel mechanism. Limnol Oceanogr 35:260–269. https://doi.org/10.4319/lo.1990.35.2.0260.
66. Barchewitz T, Guljamow A, Meissner S, Timm S, Henneberg M, Baumann O, Hagemann M, Dittmann E. 2019. Non-canonical localization of RubisCO under high-light conditions in the toxic cyanobacterium *Microcystis aeruginosa* PCC7806. Environ Microbiol 21:4836–4851. https://doi.org/10.1111/1462-2920.14837.
67. Bateson MM, Ward DM. 1988. Photoexcretion and fate of glycolate in a hot spring cyanobacterial mat. Appl Environ Microbiol 54:1738–1743. https://doi.org/10.1128/aem.54.7.1738-1743.1988.
68. Hellebust JA. 1965. Excretion of some organic compounds by marine phytoplankton. Limnol Oceanogr 10:192–206. https://doi.org/10.4319/lo.1965.10.2.0192.
69. Tolbert N. 1979. Glycolate metabolism by higher plants and algae, p 338–352. *In* Gibbs M, Latzko E (ed), Photosynthesis II. Encyclopedia of plant physiology, vol 6. Springer, Berlin, Germany.
70. Núñez MF, Pellicer MT, Badía J, Aguilar J, Baldomà L. 2001. The gene *yghK* linked to the *glc* operon of *Escherichia coli* encodes a permease for glycolate that is structurally and functionally similar to L-lactate permease. Microbiology (Reading) 147:1069–1077. https://doi.org/10.1099/00221287-147-4-1069.
71. Sinha S, Cossins E. 1965. The importance of glyoxylate in amino acid biosynthesis in plants. Biochem J 96:254–261. https://doi.org/10.1042/bj0960254.
72. Renström-Kellner E, Bergman B. 1989. Glycolate metabolism in cyanobacteria. III. Nitrogen controls excretion and metabolism of glycolate in Anabaena cylindrica. Physiol Plant 77:46–51. https://doi.org/10.1111/j.1399-3054.1989.tb05976.x.
73. But S, Egorova S, Khmelenina V, Trotsenko Y. 2019. Serine-glyoxylate aminotransferases from methanotrophs using different C1-assimilation pathways. Antonie Van Leeuwenhoek 112:741–751. https://doi.org/10.1007/s10482-018-1208-4.
74. Livshits VA, Zakataeva NP, Aleshin VV, Vitushkina MV. 2003. Identification and characterization of the new gene *rhtA* involved in threonine and homoserine efflux in *Escherichia coli*. Res Microbiol 154:123–135. https://doi.org/10.1016/S0923-2508(03)00036-6.
75. Zakataeva NP, Aleshin VV, Tokmakova IL, Troshin PV, Livshits VA. 1999. The novel transmembrane *Escherichia coli* proteins involved in the amino acid efflux. FEBS Lett 452:228–232. https://doi.org/10.1016/s0014-5793(99)00625-0.
76. Bellmann A, Vrljić M, Patek M, Sahm H, Krämer R, Eggeling L. 2001. Expression control and specificity of the basic amino acid exporter LysE of *Corynebacterium glutamicum*. Microbiology (Reading) 147:1765–1774. https://doi.org/10.1099/00221287-147-7-1765.
77. Nisbet TM, Payne JW. 1982. The characteristics of peptide uptake in *Streptococcus faecalis*: studies on the transport of natural peptides and antibacterial phosphonopeptides. J Gen Microbiol 128:1357–1364. https://doi.org/10.1099/00221287-128-6-1357.
78. Payne J, Bell G. 1979. Direct determination of the properties of peptide transport systems in *Escherichia coli*, using a fluorescent-labeling procedure. J Bacteriol 137:447–455. https://doi.org/10.1128/jb.137.1.447-455.1979.

79. Vaishampayan A. 1982. Amino acid nutrition in the blue-green alga *Nostoc muscorum*. New Phytol 90:545–549. https://doi.org/10.1111/j.1469-8137.1982.tb04487.x.
80. Neilson AH, Larsson T. 1980. The utilization of organic nitrogen for growth of algae: physiological aspects. Physiol Plant 48:542–553. https://doi.org/10.1111/j.1399-3054.1980.tb03302.x.
81. Dai R, Liu H, Qu J, Zhao X, Hou Y. 2009. Effects of amino acids on microcystin production of the *Microcystis aeruginosa*. J Hazard Mater 161:730–736. https://doi.org/10.1016/j.jhazmat.2008.04.015.
82. Goldman J, Dennett M. 1991. Ammonium regeneration and carbon utilization by marine bacteria grown on mixed substrates. Mar Biol 109:369–378. https://doi.org/10.1007/BF01313502.
83. Goldman JC, Caron DA, Dennett MR. 1987. Regulation of gross growth efficiency and ammonium regeneration in bacteria by substrate C:N ratio. Limnol Oceanogr 32:1239–1252. https://doi.org/10.4319/lo.1987.32.6.1239.
84. Gardner WS, Newell SE, McCarthy MJ, Hoffman DK, Lu K, Lavrentyev PJ, Hellweger FL, Wilhelm SW, Liu Z, Bruesewitz DA, Paerl HW. 2017. Community biological ammonium demand: a conceptual model for Cyanobacteria blooms in eutrophic lakes. Environ Sci Technol 51:7785–7793. https://doi.org/10.1021/acs.est.6b06296.
85. Banerjee R, Ragsdale SW. 2003. The many faces of vitamin B12: catalysis by cobalamin-dependent enzymes. Annu Rev Biochem 72:209–247. https://doi.org/10.1146/annurev.biochem.72.121801.161828.
86. Helliwell KE, Lawrence AD, Holzer A, Kudahl UJ, Sasso S, Kräutler B, Scanlan DJ, Warren MJ, Smith AG. 2016. Cyanobacteria and eukaryotic algae use different chemical variants of vitamin B12. Curr Biol 26:999–1008. https://doi.org/10.1016/j.cub.2016.02.041.
87. Zheng Q, Wang Y, Lu J, Lin W, Chen F, Jiao N. 2020. Metagenomic and metaproteomic insights into photoautotrophic and heterotrophic interactions in a *Synechococcus* culture. mBio 11:e03261-19. https://doi.org/10.1128/mBio.03261-19.
88. Bassford P, Bradbeer C, Kadner RJ, Schnaitman CA. 1976. Transport of vitamin B12 in tonB mutants of *Escherichia coli*. J Bacteriol 128:242–247. https://doi.org/10.1128/jb.128.1.242-247.1976.
89. Reynolds PR, Mottur GP, Bradbeer C. 1980. Transport of vitamin B12 in *Escherichia coli*. Some observations on the roles of the gene products of *BtuC* and *TonB*. J Biol Chem 255:4313–4319. https://doi.org/10.1016/S0021-9258(19)85667-3.
90. Stupperich E, Kräutler B. 1988. Pseudo vitamin B_{12} or 5-hydroxybenzimidazolyl-cobamide are the corrinoids found in methanogenic bacteria. Arch Microbiol 149:268–271. https://doi.org/10.1007/BF00422016.
91. Anderson PJ, Lango J, Carkeet C, Britten A, Kräutler B, Hammock BD, Roth JR. 2008. One pathway can incorporate either adenine or dimethylbenzimidazole as an α-axial ligand of B_{12} cofactors in *Salmonella enterica*. J Bacteriol 190:1160–1171. https://doi.org/10.1128/JB.01386-07.
92. Schnellbaecher A, Binder D, Bellmaine S, Zimmer A. 2019. Vitamins in cell culture media: stability and stabilization strategies. Biotechnol Bioeng 116:1537–1555. https://doi.org/10.1002/bit.26942.
93. Facey JA, King JJ, Apte SC, Mitrovic SM. 2021. Assessing the importance of cobalt as a micronutrient for freshwater cyanobacteria. J Phycol 58:71–79.
94. Bonnet S, Webb EA, Panzeca C, Karl DM, Capone DG, Wilhelmy SAS. 2010. Vitamin B12 excretion by cultures of the marine cyanobacteria *Crocosphaera* and *Synechococcus*. Limnol Oceanogr 55:1959–1964. https://doi.org/10.4319/lo.2010.55.5.1959.
95. Dick GJ, Duhaime MB, Evans JT, Errera RM, Godwin C, Kharbush JJ, Nitschky HS, Powers MA, Vanderploeg HA, Schmidt KC, Smith DJ, Yancey CE, Zwiers CC, Denef VJ. 2021. The genetic and ecophysiological diversity of Microcystis. Environ Microbiol 23:7278–7313. https://doi.org/10.1111/1462-2920.15615.
96. Zhu W, Li M, Luo Y, Dai X, Guo L, Xiao M, Huang J, Tan X. 2014. Vertical distribution of *Microcystis* colony size in Lake Taihu: its role in algal blooms. J Great Lakes Res 40:949–955. https://doi.org/10.1016/j.jglr.2014.09.009.
97. Chaffin JD, Davis TW, Smith DJ, Baer MM, Dick GJ. 2018. Interactions between nitrogen form, loading rate, and light intensity on *Microcystis* and *Planktothrix* growth and microcystin production. Harmful Algae 73:84–97. https://doi.org/10.1016/j.hal.2018.02.001.
98. Newell SE, Davis TW, Johengen TH, Gossiaux D, Burtner A, Palladino D, McCarthy MJ. 2019. Reduced forms of nitrogen are a driver of non-nitrogen-fixing harmful cyanobacterial blooms and toxicity in Lake Erie. Harmful Algae 81:86–93. https://doi.org/10.1016/j.hal.2018.11.003.
99. Den Uyl PA, Harrison SB, Godwin CM, Rowe MD, Strickler JR, Vanderploeg HA. 2021. Comparative analysis of *Microcystis* buoyancy in western Lake Erie and Saginaw Bay of Lake Huron. Harmful Algae 108:102102. https://doi.org/10.1016/j.hal.2021.102102.
100. Li D, Liu C-M, Luo R, Sadakane K, Lam T-W. 2015. MEGAHIT: an ultra-fast single-node solution for large and complex metagenomics assembly via succinct de Bruijn graph. Bioinformatics 31:1674–1676. https://doi.org/10.1093/bioinformatics/btv033.
101. Bushnell B. 2018. BBTools: a suite of fast, multithreaded bioinformatics tools designed for analysis of DNA and RNA sequence data. Joint Genome Institute, Berkeley, CA.
102. Berry MA, Davis TW, Cory RM, Duhaime MB, Johengen TH, Kling GW, Marino JA, Den Uyl PA, Gossiaux D, Dick GJ, Denef VJ. 2017. Cyanobacterial harmful algal blooms are a biological disturbance to Western Lake Erie bacterial communities. Environ Microbiol 19:1149–1162. https://doi.org/10.1111/1462-2920.13640.
103. Steffen MM, Davis TW, McKay RML, Bullerjahn GS, Krausfeldt LE, Stough JMA, Neitzey ML, Gilbert NE, Boyer GL, Johengen TH, Gossiaux DC, Burtner AM, Palladino D, Rowe MD, Dick GJ, Meyer KA, Levy S, Boone BE, Stumpf RP, Wynne TT, Zimba PV, Gutierrez D, Wilhelm SW. 2017. Ecophysiological examination of the Lake Erie *Microcystis* bloom in 2014: linkages between biology and the water supply shutdown of Toledo, OH. Environ Sci Technol 51:6745–6755. https://doi.org/10.1021/acs.est.7b00856.
104. Alneberg J, Bjarnason BS, De Bruijn I, Schirmer M, Quick J, Ijaz UZ, Lahti L, Loman NJ, Andersson AF, Quince C. 2014. Binning metagenomic contigs by coverage and composition. Nat Methods 11:1144–1146. https://doi.org/10.1038/nmeth.3103.
105. Kang DD, Li F, Kirton E, Thomas A, Egan R, An H, Wang Z. 2019. MetaBAT 2: an adaptive binning algorithm for robust and efficient genome reconstruction from metagenome assemblies. PeerJ 7:e7359. https://doi.org/10.7717/peerj.7359.
106. Laczny CC, Sternal T, Plugaru V, Gawron P, Atashpendar A, Margossian HH, Coronado S, Van der Maaten L, Vlassis N, Wilmes P. 2015. VizBin-an application for reference-independent visualization and human-augmented binning of metagenomic data. Microbiome 3:1. https://doi.org/10.1186/s40168-014-0066-1.
107. Dick GJ, Andersson AF, Baker BJ, Simmons SL, Thomas BC, Yelton AP, Banfield JF. 2009. Community-wide analysis of microbial genome sequence signatures. Genome Biol 10:R85. https://doi.org/10.1186/gb-2009-10-8-r85.
108. Sieber CM, Probst AJ, Sharrar A, Thomas BC, Hess M, Tringe SG, Banfield JF. 2018. Recovery of genomes from metagenomes via a dereplication, aggregation and scoring strategy. Nat Microbiol 3:836–843. https://doi.org/10.1038/s41564-018-0171-1.
109. Langmead B, Salzberg SL. 2012. Fast gapped-read alignment with Bowtie 2. Nat Methods 9:357–359. https://doi.org/10.1038/nmeth.1923.
110. Eren AM, Esen ÖC, Quince C, Vineis JH, Morrison HG, Sogin ML, Delmont TO. 2015. Anvi'o: an advanced analysis and visualization platform for 'omics data. PeerJ 3:e1319. https://doi.org/10.7717/peerj.1319.
111. Parks DH, Imelfort M, Skennerton CT, Hugenholtz P, Tyson GW. 2015. CheckM: assessing the quality of microbial genomes recovered from isolates, single cells, and metagenomes. Genome Res 25:1043–1055. https://doi.org/10.1101/gr.186072.114.
112. Olm MR, Brown CT, Brooks B, Banfield JF. 2017. dRep: a tool for fast and accurate genomic comparisons that enables improved genome recovery from metagenomes through de-replication. ISME J 11:2864–2868. https://doi.org/10.1038/ismej.2017.126.
113. Huntemann M, Ivanova NN, Mavromatis K, Tripp HJ, Paez-Espino D, Palaniappan K, Szeto E, Pillay M, Chen I-MA, Pati A, Nielsen T, Markowitz VM, Kyrpides NC. 2015. The standard operating procedure of the DOE-JGI microbial genome annotation pipeline (MGAP v.4). Stand Genomic Sci 10:86. https://doi.org/10.1186/s40793-015-0077-y.
114. Elbourne LD, Tetu SG, Hassan KA, Paulsen IT. 2017. TransportDB 2.0: a database for exploring membrane transporters in sequenced genomes from all domains of life. Nucleic Acids Res 45:D320–D324. https://doi.org/10.1093/nar/gkw1068.
115. Altschul SF, Gish W, Miller W, Myers EW, Lipman DJ. 1990. Basic local alignment search tool. J Mol Biol 215:403–410. https://doi.org/10.1016/S0022-2836(05)80360-2.
116. Pruesse E, Quast C, Knittel K, Fuchs BM, Ludwig W, Peplies J, Glöckner FO. 2007. SILVA: a comprehensive online resource for quality checked and aligned ribosomal RNA sequence data compatible with ARB. Nucleic Acids Res 35:7188–7196. https://doi.org/10.1093/nar/gkm864.

117. Pruesse E, Peplies J, Glöckner FO. 2012. SINA: accurate high-throughput multiple sequence alignment of ribosomal RNA genes. Bioinformatics 28:1823–1829. https://doi.org/10.1093/bioinformatics/bts252.
118. Wang Q, Garrity GM, Tiedje JM, Cole JR. 2007. Naive Bayesian classifier for rapid assignment of rRNA sequences into the new bacterial taxonomy. Appl Environ Microbiol 73:5261–5267. https://doi.org/10.1128/AEM.00062-07.
119. Schloss PD, Westcott SL, Ryabin T, Hall JR, Hartmann M, Hollister EB, Lesniewski RA, Oakley BB, Parks DH, Robinson CJ, Sahl JW, Stres B, Thallinger GG, Van Horn DJ, Weber CF. 2009. Introducing mothur: open-source, platform-independent, community-supported software for describing and comparing microbial communities. Appl Environ Microbiol 75:7537–7541. https://doi.org/10.1128/AEM.01541-09.
120. Wick RR, Schultz MB, Zobel J, Holt KE. 2015. Bandage: interactive visualization of de novo genome assemblies. Bioinformatics 31:3350–3352. https://doi.org/10.1093/bioinformatics/btv383.
121. Stamatakis A. 2006. RAxML-VI-HPC: maximum likelihood-based phylogenetic analyses with thousands of taxa and mixed models. Bioinformatics 22:2688–2690. https://doi.org/10.1093/bioinformatics/btl446.
122. Letunic I, Bork P. 2007. Interactive Tree Of Life (iTOL): an online tool for phylogenetic tree display and annotation. Bioinformatics 23:127–128. https://doi.org/10.1093/bioinformatics/btl529.
123. Sievers F, Wilm A, Dineen D, Gibson TJ, Karplus K, Li W, Lopez R, McWilliam H, Remmert M, Söding J, Thompson JD, Higgins DG. 2011. Fast, scalable generation of high-quality protein multiple sequence alignments using Clustal Omega. Mol Syst Biol 7:539. https://doi.org/10.1038/msb.2011.75.
124. Paver SF, Newton RJ, Coleman ML. 2020. Microbial communities of the Laurentian Great Lakes reflect connectivity and local biogeochemistry. Environ Microbiol 22:433–446. https://doi.org/10.1111/1462-2920.14862.
125. Rozmarynowycz MJ, Beall BF, Bullerjahn GS, Small GE, Sterner RW, Brovold SS, D'souza NA, Watson SB, McKay RML. 2019. Transitions in microbial communities along a 1600 km freshwater trophic gradient. J Great Lakes Res 45:263–276. https://doi.org/10.1016/j.jglr.2019.01.004.
126. Kara EL, Hanson PC, Hu YH, Winslow L, McMahon KD. 2013. A decade of seasonal dynamics and co-occurrences within freshwater bacterioplankton communities from eutrophic Lake Mendota, WI, USA. ISME J 7:680–684. https://doi.org/10.1038/ismej.2012.118.
127. Tromas N, Fortin N, Bedrani L, Terrat Y, Cardoso P, Bird D, Greer CW, Shapiro BJ. 2017. Characterising and predicting cyanobacterial blooms in an 8-year amplicon sequencing time course. ISME J 11:1746–1763. https://doi.org/10.1038/ismej.2017.58.
128. Chun S-J, Cui Y, Lee CS, Cho AR, Baek K, Choi A, Ko S-R, Lee H-G, Hwang S, Oh H-M, Ahn C-Y. 2019. Characterization of distinct cyanoHABs-related modules in microbial recurrent association network. Front Microbiol 10:1637. https://doi.org/10.3389/fmicb.2019.01637.
129. Miller CS, Baker BJ, Thomas BC, Singer SW, Banfield JF. 2011. EMIRGE: reconstruction of full-length ribosomal genes from microbial community short read sequencing data. Genome Biol 12:R44. https://doi.org/10.1186/gb-2011-12-5-r44.
130. Allen MM, Stanier RY. 1968. Selective isolation of blue-green algae from water and soil. J Gen Microbiol 51:203–209. https://doi.org/10.1099/00221287-51-2-203.
131. Heal KR, Carlson LT, Devol AH, Armbrust EV, Moffett JW, Stahl DA, Ingalls AE. 2014. Determination of four forms of vitamin B12 and other B vitamins in seawater by liquid chromatography/tandem mass spectrometry. Rapid Commun Mass Spectrom 28:2398–2404. https://doi.org/10.1002/rcm.7040.